

THE SAHARAN AEROSOL LONG-RANGE TRANSPORT AND AEROSOL–CLOUD-INTERACTION EXPERIMENT

Overview and Selected Highlights

BERNADETT WEINZIERL, A. ANSMANN, J. M. PROSPERO, D. ALTHAUSEN, N. BENKER, F. CHOUZA, M. DOLLNER, D. FARRELL, W. K. FOMBA, V. FREUDENTHALER, J. GASTEIGER, S. GROß, M. HAARIG, B. HEINOLD, K. KANDLER, T. B. KRISTENSEN, O. L. MAYOL-BRACERO, T. MÜLLER, O. REITEBUCH, D. SAUER, A. SCHÄFLER, K. SCHEPANSKI, A. SPANU, I. TEGEN, C. TOLEDANO, AND A. WALSER

The aircraft and ground-based SALTRACE campaign in the tropical Atlantic in 2013/14 characterized the large-scale transport of African dust, dust “aging” during transit, and its impact on radiation and cloud microphysics.

Although substantial effort has been undertaken in the last decades to improve our knowledge about the role of aerosols in the climate system, aerosols and clouds still pose the largest uncertainty to estimates and interpretations of Earth’s changing energy budget (IPCC 2013). Among aerosols, mineral dust particles (herein, simply “dust particles” or “dust”) are of key importance because they contribute to about half of the global annual particle emissions by mass (Hinds 1999; Huneus et al. 2011); significantly impact the radiation budget of Earth by scattering, absorption, and emission of solar and terrestrial radiation (Sokolik et al. 2001; Tegen 2003; Balkanski et al. 2007); act as cloud condensation nuclei (CCN); and have been identified as effective ice nucleating particles (INP; Hoose and Möhler 2012). Deposited dust can be a significant nutrient to the ocean (Jickells et al. 2005; Maher et al.

2010; Niedermeier et al. 2014). In addition, dust may have a severe impact on aviation by causing poor visibility (Weinzierl et al. 2012) affecting the takeoff and landing of aircraft. Last but not least, there is increasing evidence that dust might be a human health concern (Goudie 2014; Morman and Plumlee 2014).

The major dust source regions are located in the Northern Hemisphere and extend from the west coast of North Africa, through the Middle East, to Central Asia and China. Aerosol Comparisons between Observations and Models (AeroCom) simulations estimate that North Africa including the Sahara emits about 200–3,000 Tg of dust every year, thereby contributing about 70% to the total global dust emission (Huneus et al. 2011). African dust is regularly transported westward across the Atlantic Ocean to the Caribbean (e.g., Prospero 1999; Prospero and Lamb 2003; Stevens et al. 2016), the southern United States (Prospero 1999), and northeastern South America (Swap et al. 1992; Prospero et al. 2014).

Publisher’s Note: On 25 July 2017 this article was revised to correct an in-text citation for Walser et al. (2017).

During the summer months the main dust transport takes place in the Saharan air layer (SAL), a hot, dry, elevated layer that has its origins over the Sahara Desert (Carlson and Prospero 1972; Prospero and Carlson 1972). The SAL often covers large parts of the tropical Atlantic Ocean and can be easily tracked by satellite observations of aerosol optical depth (AOD) and lidar (e.g., Liu et al. 2008; Chouza et al. 2016a). Presently, the SAL is attracting great interest because it is suspected to influence tropical cyclone activity (e.g., Dunion and Velden 2004; Braun 2010; Evan et al. 2011; Peng et al. 2012; Brammer and Thorncroft 2015; Hanks et al. 2015). However, the details of this influence are not yet understood.

In the past decade several comprehensive airborne dust field experiments including the Saharan Mineral Dust Experiment (SAMUM-1, Heintzenberg 2009; SAMUM-2, Ansmann et al. 2011) were performed in the vicinity of the Sahara and in the outflow region of African dust in the Cabo Verde area. Table 1 and references therein give an overview over major airborne dust field experiments over Africa, the Atlantic Ocean, and in the Caribbean. Although a few airborne dust campaigns focused on the Caribbean, most of these previous measurements in the Caribbean only covered altitudes below 3 km, and they lacked the extensive instrumentation available to us in the Saharan Aerosol Long-Range Transport and Aerosol–Cloud-Interaction Experiment (SALTRACE). Recent ground-based measurements at the Caribbean island of Puerto Rico studied African dust size distribution, optical properties, dust-cloud impacts (Spiegel et al. 2014; Raga et al. 2016), and chemical composition (Gioda et al. 2013;

Denjean et al. 2015; Fitzgerald et al. 2015; Denjean et al. 2016; Valle-Diaz et al. 2016).

Despite substantial progress, many questions concerning the role of dust in the climate system remain open (e.g., Ansmann et al. 2011; Ryder et al. 2015). For example, the uncertainty of Intergovernmental Panel on Climate Change (IPCC) Assessment Report 5 estimates for global average direct radiative forcing by anthropogenic mineral dust aerosol that is assumed to be 20% of total dust is $[-0.3; +0.1] \text{ Wm}^{-2}$ (Table 8.4 in Myhre et al. 2013). This range has not changed since the previous IPCC report in 2007, indicating further research needs.

A critical parameter for the derivation of radiative forcing estimates is the particle size distribution that is set at emission (Mahowald et al. 2014), but changes during long-range transport. For example, preferably large supermicron dust particles are lost through gravitational settling and efficient particle aging occurs when particles act as CCN and INP (Pöschl 2005). Cloud processing is one possible pathway producing sulfate-coated dust particles and changing the aerosol size spectrum (e.g., Levin et al. 1996; Wurzler et al. 2000), thus changing the probability of rain formation and influencing wet deposition of dust. Recent laboratory measurements indicate that dust particles may become better CCN after cloud processing (Kumar et al. 2011). Understanding the very complex interaction between aerosols, clouds, and precipitation is challenging and requires comprehensive, coordinated, and long-term measurements and state-of-the-art modeling (Stevens and Feingold 2009). Many models have attempted to simulate the effects of aging (e.g., Abdelkader et al. 2015), but it is difficult to assess the validity of these results because of the absence of data with which to test the effect.

AFFILIATIONS: WEINZIERL AND SPANU—Universität Wien (UNIVIE), Fakultät für Physik, Aerosolphysik und Umweltphysik, Wien, Austria, and Institut für Physik der Atmosphäre, Deutsches Zentrum für Luft- und Raumfahrt (DLR), Oberpfaffenhofen, Germany; ANSMANN, ALTHAUSEN, FOMBA, HAARIG, HEINOLD, KRISTENSEN, MÜLLER, SCHEPANSKI, AND TEGEN—Leibniz Institute for Tropospheric Research (TROPOS), Leipzig, Germany; PROSPERO—University of Miami, Miami, Florida; BENKER AND KANDLER—Institut für Angewandte Geowissenschaften, Technische Universität Darmstadt, Darmstadt, Germany; CHOUZA, GROß, REITEBUCH, SAUER, AND SCHÄFLER—Institut für Physik der Atmosphäre, Deutsches Zentrum für Luft- und Raumfahrt (DLR), Oberpfaffenhofen, Germany; DOLLNER AND GASTEIGER—Universität Wien (UNIVIE), Fakultät für Physik, Aerosolphysik und Umweltphysik, Wien, Austria, and Ludwig-Maximilians-Universität (LMU), Meteorologisches Institut, München, Germany; FARRELL—Caribbean Institute for Meteorology and Hydrology (CIMH), Bridgetown, Barbados; FREUDENTHALER—Ludwig-Maximilians-Universität (LMU), Meteorologisches Institut, München, Germany;

MAYOL-BRACERO—Department of Environmental Science, University of Puerto Rico, San Juan, Puerto Rico; TOLEDANO—Grupo de Óptica Atmosférica, Universidad de Valladolid, Valladolid, Spain; WALSER—Ludwig-Maximilians-Universität (LMU), Meteorologisches Institut, München, and Institut für Physik der Atmosphäre, Deutsches Zentrum für Luft- und Raumfahrt (DLR), Oberpfaffenhofen, Germany
CORRESPONDING AUTHOR: Bernadett Weinzierl, bernadett.weinzierl@univie.ac.at

The abstract for this article can be found in this issue, following the table of contents.

DOI:10.1175/BAMS-D-15-00142.1

A supplement to this article is available online (10.1175/BAMS-D-15-00142.2)

In final form 21 November 2016

©2017 American Meteorological Society

For information regarding reuse of this content and general copyright information, consult the [AMS Copyright Policy](#).

In a recent review, Mahowald et al. (2014) concluded that new measurements of dust size distributions agree roughly within the size range between 0.1- and 5- μm particle diameters, but below and above this size range, the dust size distribution is not well understood. In particular, it is not clear why in situ observations generally lead to considerably larger mean particle sizes than retrievals from remote sensing instruments (Reid et al. 2003a; Müller et al. 2010; Toledano et al. 2011). This is particularly important for radiative forcing estimates, as the coarse mode size distribution has a strong impact on the radiative budget and can even switch the sign of the radiative forcing from a net cooling to heating (Otto et al. 2007).

These various studies demonstrate that dust is associated with a significant climate effect and may have a substantial impact on cloud processes and, furthermore, that particle aging might enhance these effects. We lack the understanding of the processes that lead to mixing of dust with other aerosols and of the factors that affect dust deposition.

In SALTRACE we collected a unique dataset that provides new insights into these processes. This article presents an overview of the SALTRACE program and highlights important results. In “Overview of the SALTRACE project,” we introduce the SALTRACE measurement sites, intensive observation periods, and instrumentation. The remaining sections respectively evaluate the SALTRACE measurements in the context of the 50-yr Barbados dust record, describe the dust source activity during SALTRACE and follow with the conceptual “big picture” of transatlantic dust transport, and highlight selected SALTRACE results including the modification of dust during transatlantic transport, the passage of Tropical Storm Chantal and its impact on the dust layer structure, and dust as a reservoir/source for CCN and INP.

OVERVIEW OF THE SALTRACE PROJECT.

SALTRACE (www.pa.op.dlr.de/saltrace) was conducted from spring 2013 through summer 2014. Table 2 gives an overview of activities performed within the SALTRACE framework. The core of the SALTRACE program was an atmospheric column closure experiment¹ in June and July 2013 involving ground-based and airborne in situ and remote sensing observations in Barbados (main supersite), Puerto Rico, and Cabo Verde. For the airborne SALTRACE

measurements, the Deutsches Zentrum für Luft- und Raumfahrt (DLR) research aircraft Falcon was equipped with a suite of in situ instruments for the determination of microphysical and optical aerosol properties, and with sampling devices for offline particle analysis, a nadir-looking 2- μm wind lidar, dropsondes, and instruments for standard meteorological parameters. Details about the instrumentation at the main supersite in Barbados and on the research aircraft as well as accompanied modeling activities at large-eddy and regional scale are given in Table ES1 of the supplemental material (<http://dx.doi.org/10.1175/BAMS-D-15-00142.2>). Before the measurements in June and July 2013, a cruise of the Research Vessel *Meteor* between Guadeloupe and Cabo Verde took place in April and May 2013 (Kanitz et al. 2014). Later, in February and March 2014 (SALTRACE-2) and June and July 2014 (SALTRACE-3), additional intensive ground-based lidar and sun photometer observations followed to cover the annual variability of dust flow into the Caribbean (Table 2).

Figure 1 sketches the airborne SALTRACE observations in summer 2013 including flight tracks (red lines). Figure 2 shows the Falcon base at Grantley International Airport together with the measurement locations of the in situ and remote sensing measurements on Barbados. In total, 31 research flights were performed. The DLR research aircraft Falcon spent more than 86 of a total of 110 flight hours studying dust from several dust outbreaks under a variety of atmospheric conditions between Senegal, Cabo Verde, the Caribbean, and Florida.

A detailed list of SALTRACE flights including takeoff time, landing time, and objective is provided in the supplemental material (Table ES2). The flights in the Cabo Verde region (11–17 June 2013) aimed to characterize dust close to the source region and are also used for comparison with data from SAMUM-2 measurements (January and February 2008) in the Cabo Verde area (Ansmann et al. 2011; Weinzierl et al. 2011; references therein). The first part of the research flights in the Caribbean (20–26 June 2013) studied the horizontal variability of dust properties with extended east–west and north–south sampling flights and included the transatlantic dust sampling of the same air mass on both sides of the Atlantic (17 and 22 June 2013). The flights on 30 June and 1 July were intended to investigate the variability of dust properties between Barbados, Antigua, and Puerto Rico and to study the wet deposition of dust. The second half of the measurements (5–12 July 2013) focused on extended vertical profiling over the Atlantic east of Barbados, over the lidar and

¹ Atmospheric column closure experiments aim to characterize the same parameters of a system with different, independent methods and models to minimize the measurement uncertainties through comparison of the derived values.

TABLE 1. Overview of airborne mineral dust field experiments near the dust sources over Africa, the Atlantic Ocean, and in the Caribbean mainly focusing on the past two decades. AMMA-SOP0: African Monsoon Multidisciplinary Analysis–Special Observation Period 0; BACEX: Barbados Aerosol Cloud Experiment; BOMEX: Barbados Oceanic and Meteorological Experiment; CARRIBA: Cloud, Aerosol, Radiation and Turbulence in the Trade Wind Regime over Barbados; CRYSTAL-FACE: Cirrus Regional Study of Tropical Anvils and Cirrus Layers—Florida-Area Cirrus Experiment; DABEX: Dust and Biomass-Burning Experiment; DODO: Dust Outflow and Deposition to the Ocean; Fennec: not an acronym; GERBILS: Geostationary Earth Radiation Budget Intercomparison of Longwave and Shortwave Radiation; ICE-D: Ice in Cloud Experiments—Dust; NAMMA: NASA AMMA; PRIDE: Puerto Rico Dust Experiment; SAMUM: Saharan Mineral Dust Experiment; SHADE: Saharan Dust Experiment.

Campaign acronym	Time span	Region	Objective/science focus	Overview
Field experiments near the dust sources/Africa				
SAMUM-1	May and Jun 2006	Southern Morocco	Characterize Saharan aerosol near the source region and quantify dust-related radiative effects	Heintzenberg (2009)
AMMA-SOP0	Jan and Feb 2006	West Africa	Characterize Saharan aerosol and biomass-burning aerosols from West Africa	Redelsperger et al. (2006)
DABEX	Jan and Feb 2006	Niger	Same topic as AMMA-SOP0	Haywood et al. (2008)
DODO	Feb and Aug 2006	West Africa	Characterize Saharan dust in two seasons, constrain model simulations, quantify deposition of iron to the North Atlantic Ocean	McConnell et al. (2008)
GERBILS	Jun 2007	North Africa	Geographic distribution and physical and optical properties of Saharan dust, impact on radiation, validation of satellite retrievals and numerical weather prediction models	Haywood et al. (2011)
FENNEC	Apr and Jun 2011, Jun 2012	Algeria and Mauritania	Improve understanding of the Saharan climate system through a synergy of observations and modeling	Washington et al. (2012); Ryder et al. (2015)
Atlantic Ocean off the coast of Africa				
SHADE	Sep 2000	Cabo Verde	Investigation of aerosol parameters relevant for the determination of the direct radiative effect	Tanré et al. (2003)
NAMMA	Aug–Sep 2006	Cabo Verde	Improve understanding of the relationship between the African easterly waves, the SAL, and tropical cyclogenesis	Zipser et al. (2009)
SAMUM-2	Jan and Feb 2008	Cabo Verde	Characterize Saharan aerosol and biomass-burning aerosol over the eastern Atlantic	Ansmann et al. (2011)
SAMUM-2b	May and Jun 2008	Cabo Verde	Same as SAMUM-2, but summer measurements	Ansmann et al. (2011)
SALTRACE	Apr–Jul 2013, see Table 2	Cabo Verde	Characterize dust properties before long-range transport with the same instrumentation as over the Caribbean	This study
ICE-D	Aug 2015	Cabo Verde	Study influence of mineral dust on clouds and improve representation of dust-produced INP and CCN in models	Cotton (2016)
Caribbean				
BOMEX	May–Jul 1969	Barbados	Measure vertical distribution of Saharan dust in the Caribbean and quantify dust transport over Atlantic	Prospero and Carlson (1972)
PRIDE	Jun and Jul 2000	Caribbean	Understand the issues of dust transport and radiative forcing in the subtropical North Atlantic Ocean	Reid et al. (2003b)
CRYSTAL-FACE	Jul 2002	Southern Florida	Investigate ice nucleation potential of long-range transported Saharan dust	Sassen et al. (2003)
BACEX	Mar and Apr 2010	Barbados	Observe cloud–aerosol interactions	Jung et al. (2013)

CARIBBA	Nov 2010 and Apr 2011	Barbados	High-resolution and collocated measurements of trade wind cumuli and aerosol to characterize aerosol–cloud interactions	Siebert et al. (2013)
SALTRACE	2013/14, see Table 2	Barbados and Caribbean	Characterize properties of aged dust in the Caribbean, quantify the impact of “aging” on the radiation budget and cloud microphysical processes, investigate the meteorological context of transatlantic dust transport, and assess the roles of removal processes during transport	This study

ground sites on Barbados, and west of the Caribbean islands to study downwind transport from Barbados and island effects (Chouza et al. 2016b; Jähn et al. 2016). Furthermore, we had the unique opportunity to make measurements before, during, and after the passage of Tropical Storm Chantal (8–10 July 2013). To our knowledge, these are the first measurements of dust conditions in the vicinity of such a storm ever made with an extensive aerosol instrument package. A second sequence of dust sampling flights was performed toward Puerto Rico and into the Bahamas–Florida area (11–13 July 2013). The flight program culminated with a route that took the Falcon along the East Coast of the United States, across the high-latitude North Atlantic, and back to our home base in Germany. During the flights back to Germany, the Falcon encountered thick smoke layers where refractory black carbon mass mixing ratios reached values as high as 100–380 ng kg⁻¹, higher than the values around 270 ng kg⁻¹ observed in an intense smoke layer in the upper troposphere over Germany originating from the pyroconvective Pagami Creek fire (Minnesota, United States) (Dahlkötter et al. 2014).

SALTRACE IN THE CONTEXT OF THE 50-YR BARBADOS DUST RECORD.

Barbados was chosen as main supersite for SALTRACE because it is the easternmost island of the Caribbean which enables measurements of undisturbed African dust layers after they transit the Atlantic. Furthermore, Barbados has the world’s longest record of ground-based dust measurements, which started in 1965 and continues today (Prospero and Lamb 2003; Prospero et al. 2014), allowing us to evaluate the SALTRACE data in long-term context.

Dust transport follows a pronounced seasonal cycle with a minimum in winter and a maximum in summer peaking in June–August (Doherty et al. 2008; Prospero et al. 2014). Figure 3 depicts average summer (June–August) dust mass concentration values measured at Ragged Point, Barbados, between 1965 and 2013.

The years of the SAMUM and SALTRACE measurements are indicated in red. Average summer dust mass concentrations vary from less than 10 to around 50 μg m⁻³ from year to year. The periods of high dust concentrations in the early 1970s and in the mid-1980s were linked to drought conditions in Africa (Prospero and Lamb 2003; Prospero et al. 2014), and the variability of the winds over the Sahara has been shown to impact in the dust load over the Atlantic (Wang et al. 2015; Evan et al. 2016). The causes of the variation in dust transport since the 1980s are still a subject of research and numerous efforts have been made to relate the Barbados dust record to various climate indices—for example, El Niño–Southern Oscillation (ENSO) (Prospero and Lamb 2003; DeFlorio et al. 2016), North Atlantic Oscillation (NAO) (Ginoux et al. 2004; Evan et al. 2006), and Atlantic Multidecadal Oscillation (AMO) (Evan et al. 2011; Wang et al. 2012; DeFlorio et al. 2016). Of these the AMO seems to have played a particularly strong role. However, it is notable that high concentrations in 1997/98 were coincident with an exceptionally strong El Niño. Since about 1970, excepting the periods of high concentration in summer, low summer-mean values seem to fall between 15 and 20 μg m⁻³, which might be thought of as a “background” value range. The mean value of 21 μg m⁻³ during SALTRACE is slightly above in this range. Thus, measurements made during SALTRACE could be regarded as being representative of “normal” dust conditions.

Figure 4 shows time series of AOD (black crosses) measured with Aerosol Robotic Network (AERONET; <http://aeronet.gsfc.nasa.gov/>) sun photometers at Cabo Verde, Barbados, and Puerto Rico throughout the main SALTRACE period. It illustrates the dust layer at Barbados with a time–height cross section of volume linear depolarization ratio (VLDR; for details, see discussion of Fig. 6). Maximum AOD (500 nm) detected with the sun photometers reached values of 0.85 at Cabo Verde, 0.61 at Barbados, and 0.56 at Puerto Rico during SALTRACE. The ground-based lidar measurements at Barbados showed that mineral dust contributed about 50%–70% of the total AOD at 532 nm (Groß et al. 2015). The red triangles in Fig. 4 indicate the median AOD (500 nm) during the 3–4-h duration of the individual Falcon flights, which fell into the ranges 0.5–0.8 for flights in the Cabo Verde area and 0.1–0.5 for flights in the Caribbean. The Ångström exponent of the AOD at the Barbados site (not shown) was around 0.2 on most days except for very clean (dust free) days where it increased to 0.5.

Most Falcon flights were performed during high-dust-concentration conditions, but some flights

also focused on low-dust conditions. Figure 4 shows surface-level dust mass concentration at Ragged Point (blue dots) [see Kristensen et al. (2016) for more details on ground-based measurements during SALTRACE]. The dust mass concentration was derived from spectral absorption coefficients measured with a spectral optical absorption photometer (SOAP; Müller et al. 2009) by fitting spectral mass absorption coefficients between wavelengths 425 and 675 nm to

the measurements following a reanalysis of data from Müller et al. (2009) and Schladitz et al. (2009).

The temporal trends of AOD and dust concentration at the ground agree well indicating that 1) dust makes a major contribution to the AOD in the Caribbean, 2) dust transported at higher altitudes into the Caribbean in the SAL is effectively mixed down into the boundary layer over Barbados, and 3) we can expect good comparability between ground-based,

TABLE 2. Airborne, ground-based, and shipborne measurements in the context of SALTRACE.			
Activity	Time	Observations, location	Aerosol layering
METEOR-cruise	29 Apr–23 May 2013	Shipborne lidar, Guadeloupe–Cabo Verde	Dust above marine
SALTRACE	10 Jun–15 Jul 2013	SALTRACE column experiment (ground-based and airborne in situ and remote sensing observations); for measurement locations see Fig. 1	Dust above marine
SALTRACE-2	15 Feb–8 Mar 2014	Ground-based lidar and sun photometers, Barbados	Smoke/dust above marine
SALTRACE-3	19 Jun–12 Jul 2014	Ground-based lidar and sun photometers, Barbados	Dust above marine

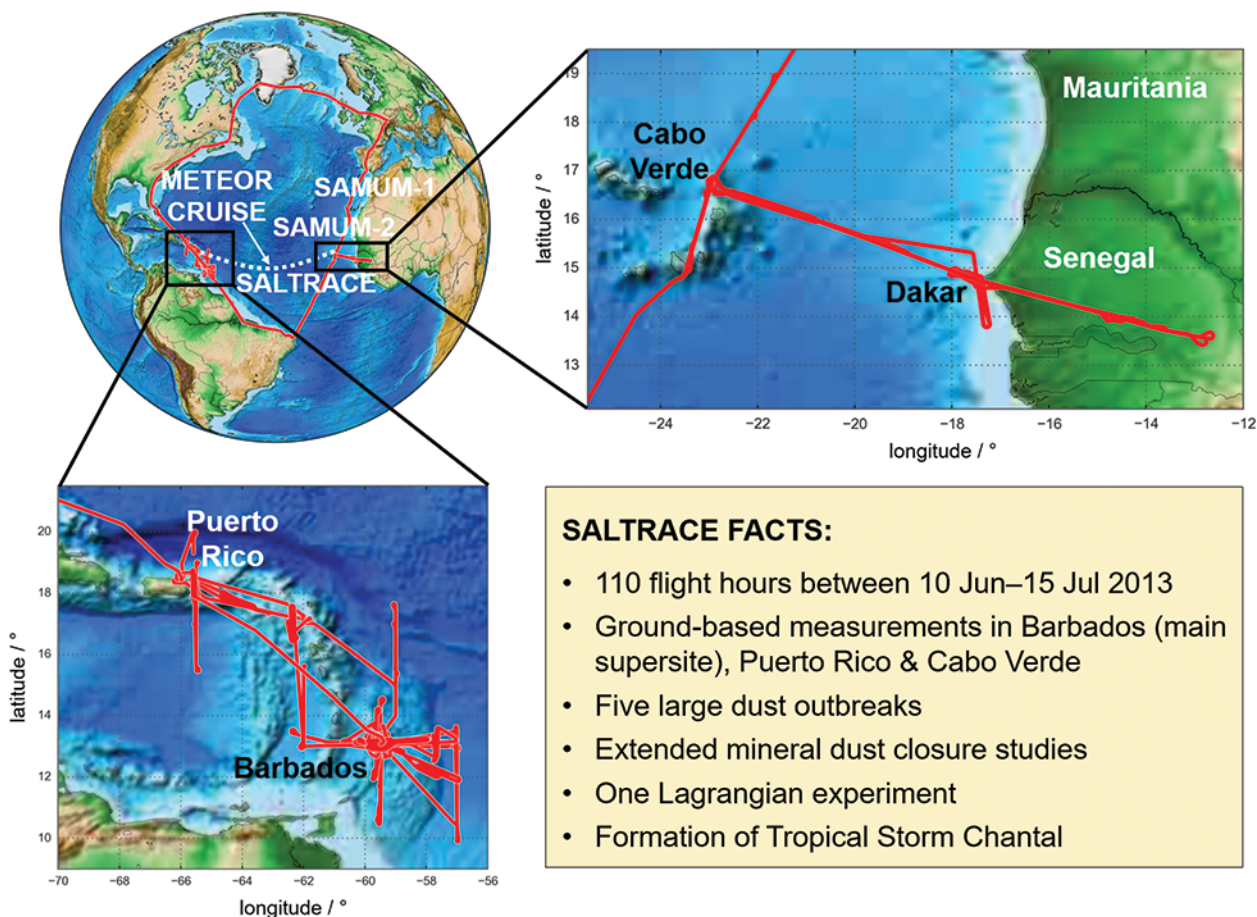


FIG. 1. Flight tracks (red lines) of the airborne SALTRACE observations (note: no data are available in Brazilian airspace) in summer 2013 with the ground sites in Barbados (main supersite), Cabo Verde, and Puerto Rico indicated. Furthermore, the locations of the SAMUM measurements in Morocco (2006) and Cabo Verde (2008) are shown.

airborne, and remote sensing observations (see also Fig. 12). Previously, Smirnov et al. (2000) had shown that monthly means of AOD and ground-based dust concentrations were highly correlated at Barbados. Our results show a good correlation on a daily basis.

DUST SOURCE ACTIVITY DURING SALTRACE. Various sources across North Africa

contribute to the dust load in the Caribbean. Figure 5 summarizes the most active dust sources for SALTRACE, SAMUM-1, and SAMUM-2. The dust source activity (DSA) was inferred from infrared dust index images calculated from brightness temperature measurements by the Spinning Enhanced Visible and Infrared Imager (SEVIRI) on board the Meteosat Second Generation (MSG) satellite

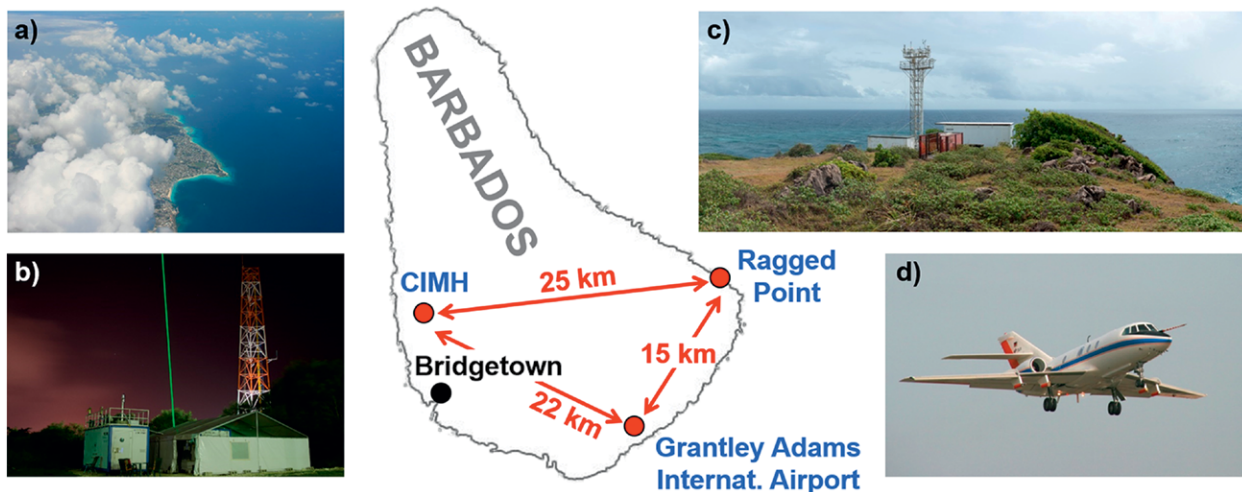


FIG. 2. Map with SALTRACE measurement locations on Barbados. (a) Photograph of trade wind cumuli over Barbados that were frequently observed. (b) Lidar and sun photometer container at Caribbean Institute for Hydrology and Meteorology, Barbados (13°8'55"N, 59°37'29"W). The green line is the laser beam from the TROPOS lidar instrument. (c) Measurement tower with the ground-based in situ measurements at Ragged Point (13°09'54"N, 59°25'56"W). (d) The DLR Falcon research aircraft taking off at Barbados (13°4'32"N, 59°29'30"W) on 20 Jun 2013.

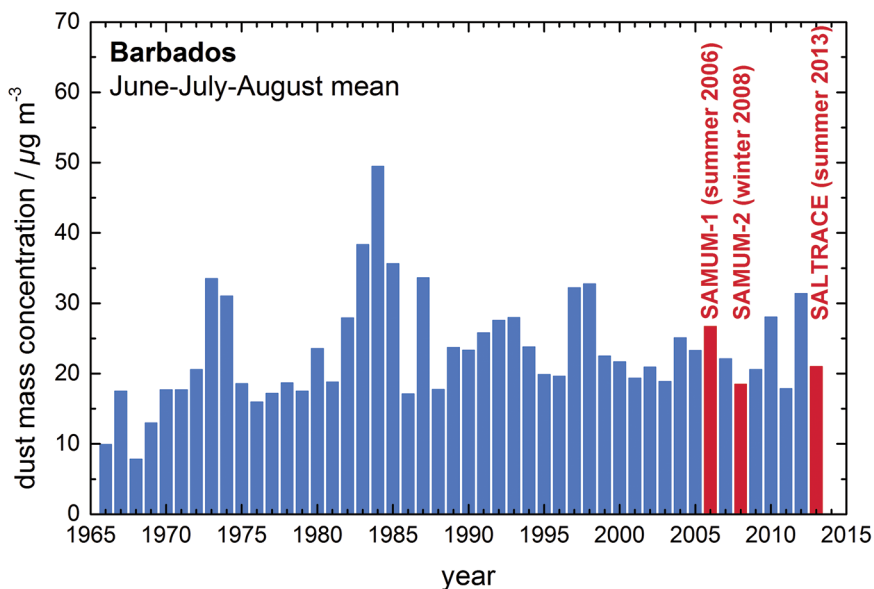


FIG. 3. Summer (Jun–Aug)-mean dust concentrations at Barbados from 1965 to 2013 with the years of the airborne field experiments SAMUM and SALTRACE indicated.

(Schepanski et al. 2007, 2009, 2012). For each of the three field campaigns, daily maps of DSA were summarized and occurrence frequencies of DSA were calculated (Fig. 5). Areas showing a DSA frequency

above the 97th percentile for the corresponding time period were colored. The gray-shaded areas indicate all source regions that were active during SALTRACE. Although seasonal and thus campaign-

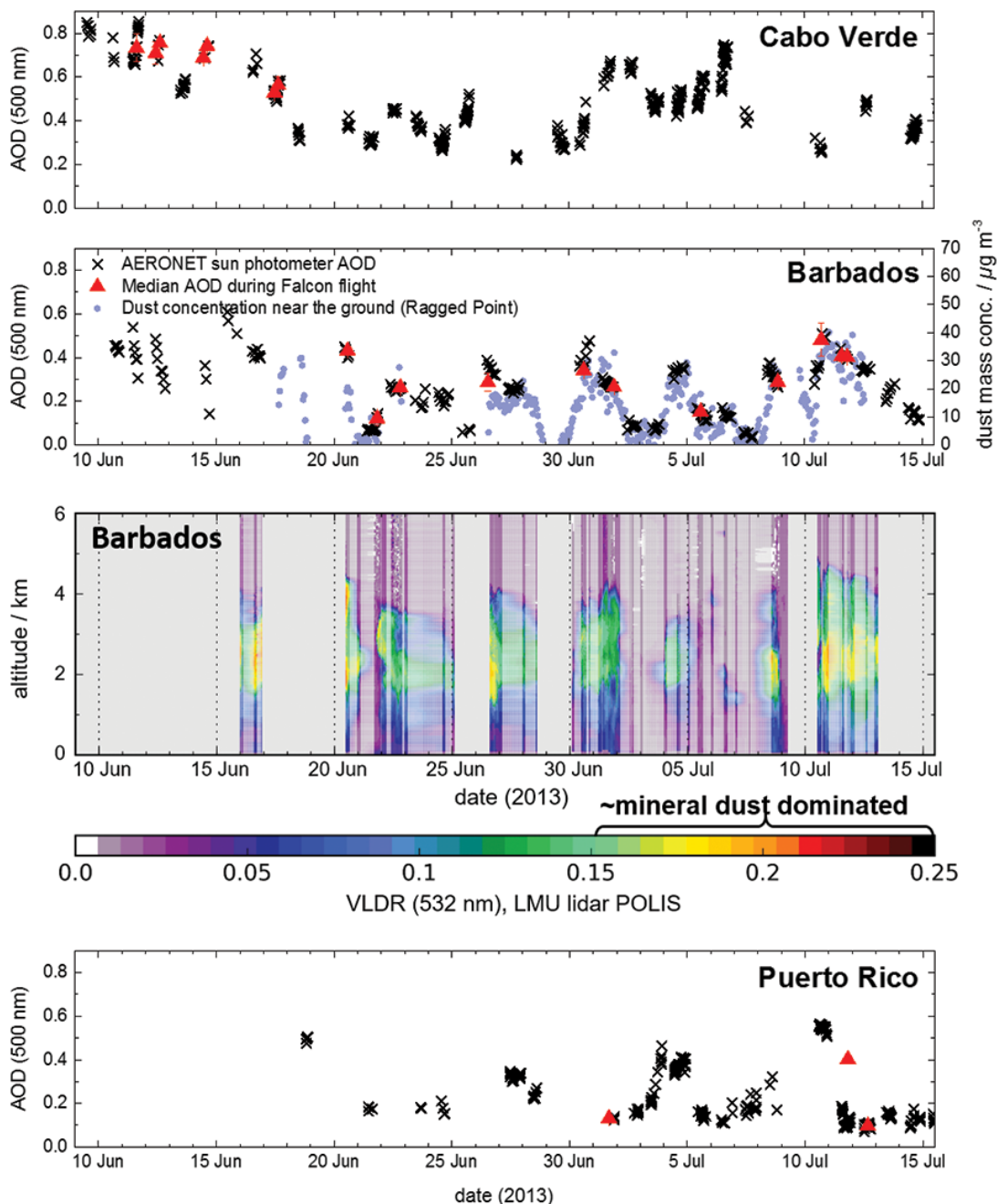


FIG. 4. AOD (500 nm) throughout SALTRACE at Cabo Verde, Barbados, and Puerto Rico together with a time–height cross section of VLDR (532 nm) illustrating the dust layer at Barbados. The red triangles in the three time series indicate the median AOD during the duration of the Falcon flights. For Barbados, also the dust mass concentration near the ground at Ragged Point is shown (blue circles). Lidar sequences in which clouds shielded the dust layer were removed. To better visualize the time evolution of the dust layer, the lidar data were linearly interpolated in periods without data. Interpolation was only performed if AOD time series suggested that no major changes were taking place. White-shaded areas mark interpolated sequences.

related differences in the pattern distribution of frequent DSA are apparent, dust sources located in the Adrar–Hoggar–Air mountain region as well as the Bodélé Depression region were predominantly active throughout all three campaigns. Dust source hot spots over the northern part of the Sahara and the Maghreb region were predominantly active during SAMUM-1 (May and June) and SALTRACE (June and July), suggesting that these regions are of additional importance in late spring and early summer.

Dust from the most active sources during SALTRACE identified in Fig. 5 is expected to have a high kaolinite and low illite abundance, as well as low calcium and high total iron contents (Scheuven et al. 2013; Nousiainen and Kandler 2015). The ratio of oxide to total iron is estimated to be higher for Bodélé and Hoggar than for Mali sources (Formenti et al. 2014). In contrast, the less active sources in the northern Sahara would be dominated by illite and exhibit higher calcite contents. Except for Bodélé, the most active sources have a generally high iron oxide content. The dust therefore is expected to contribute considerably to shortwave radiation absorption. It is particularly expected to dominate absorption for supermicron particles (Müller et al. 2009). Furthermore, their comparatively high feldspar content (Nickovic et al. 2012) might influence the specific ice nucleation ability (Atkinson et al. 2013).

THE BIG PICTURE: MINERAL TRANSPORT FROM AFRICA INTO THE CARIBBEAN.

The large-scale features of dust transport from Africa across the Atlantic were initially described in the early 1970s (Prospero et al. 1970; Carlson and Prospero 1972; Schütz 1980), but the modification of dust properties during long-range transport is still an open question. After emission over Africa, the warm, dry, and dust-containing SAL leaves the African continent and travels westward at a speed of about 1,000 km day⁻¹, crossing to Barbados in about 5 days (e.g., Huang et al. 2010). Within the course of the year, the main transport corridor for the dust outflow from Africa exhibits a south–north

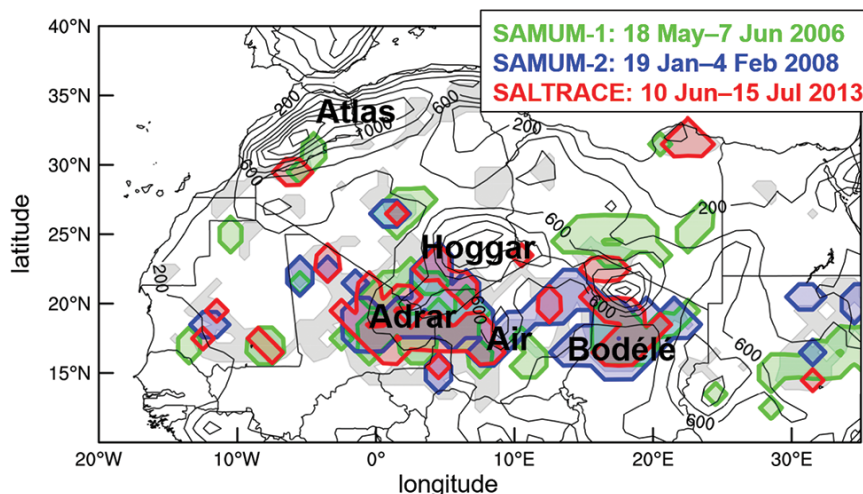


FIG. 5. Regions of most active dust sources during SALTRACE (red contours), SAMUM-1 (green contours), and SAMUM-2 (blue contours). The gray-shaded areas indicate all source regions active during SALTRACE regardless of their emission intensity and activation frequency. Solid contour lines represent the topography with altitudes (m above sea level) indicated.

migration related to the seasonal displacement of the Hadley cell in general and the cycle of the complex West African circulation in particular, in which the African easterly jet and its disturbances, so-called African easterly waves (AEWs), play an important role (e.g., Thorncroft and Blackburn 1999; Kiladis et al. 2006; Knippertz and Todd 2010). In June and July, the center of the dust corridor and the largest AOD is found between 15° and 20°N transporting mineral dust into the Caribbean and toward Florida, whereas in winter, the dust corridor is centered between 5° and 10°N and the dust extends to South America (Schütz 1980; Huang et al. 2010; Yu et al. 2015).

As visible in Fig. 4, dust concentrations in Barbados have a pulsating nature that is connected to the passage of AEWs (Carlson and Prospero 1972), which periodically interrupt the dust flow into the Caribbean and occasionally intensify into tropical cyclones (Zipser et al. 2009). The passage of AEWs is associated with moist air, cloudiness, and precipitation. Dust events appear to follow behind AEWs (Karyampudi and Carlson 1988).

The structure and vertical distribution of the mineral dust layer changes during transit. Figure 6 (top) shows these changes by means of cross sections of backscatter from the airborne wind lidar system on board the Falcon (Chouza et al. 2015; Chouza et al. 2016a). The bottom panel of Fig. 6 sketches the changes in dust layer structure and also the processes modifying the size distribution of the dust aerosol. Over West Africa, dust extends from the surface to 6–7-km altitude (e.g., Schütz 1980; Weinzierl

et al. 2009). When leaving the African continent, the dust-containing continental outflow overrides the cool dust-free trade winds to form the elevated SAL (Weinzierl et al. 2009, 2011; Khan et al. 2015). In the Cabo Verde region, the lidar shows a homogenous dust layer extending above the trade wind inversion from about 1.5- to 6–7-km altitude (Fig. 6, top). During transit, the top of the SAL descends from 6–7 km over West Africa to 4–5 km in the Caribbean with an average of $\sim 0.4\text{--}0.6\text{ km day}^{-1}$. Dust is transferred from the SAL to the marine boundary layer by entrainment at the top of the marine boundary layer, via turbulent and convective downward mixing, and by gravitational settling of mainly supermicron particles leading to changes in the dust size distribution. In addition, cloud processing, dilution, and wet deposition are expected to modify aerosol properties in the SAL in the course of transport.

The vertical layering described in Fig. 6 is typical for summer. Figure 7 illustrates the variability and seasonal differences in vertical structure based on ground-based lidar observations with the Backscatter Extinction Lidar-Ratio Temperature Humidity Profiling Apparatus (BERTHA) (Haarig et al. 2016; Haarig et al. 2017, manuscript submitted to *Atmos. Chem. Phys.*) from the Leibniz Institute for Tropospheric Research (TROPOS) at three different locations between Africa and the Caribbean in

summer 2006, 2008, 2013, and 2014 and in winter 2008 and 2014. The six panels depict time–altitude cross sections of the VLDR at wavelengths of 710 and 1,064 nm, respectively. The VLDR is derived from the ratio of the measured cross-polarized to copolarized component in the backscattered light when linearly polarized light is emitted by the laser. This quantity includes the contribution from both, molecules and particles. From the VLDR, the linear depolarization ratio of particles (PLDR) can be derived, which serves to identify aerosol types (e.g., Tesche et al. 2009, 2011; Weinzierl et al. 2011; Burton et al. 2012; Groß et al. 2013). Regions with predominantly aspherical particles of pure dust (PLDR of $31\% \pm 3\%$ at 532 nm; Freudenthaler et al. 2009) appear in red. Marine aerosol with mostly spherical particles (PLDR of $2\% \pm 1\%$ at 532 nm for relative humidities greater than 50%; Groß et al. 2011) are shown in blue. Mixtures of dust particles with spherical particles (e.g., marine aerosol at high relative humidity but also biomass particles) appear as yellow-greenish colors (Tesche et al. 2009).

In all cases, the aerosol layers extend from the ground up to altitudes between 3 and 5 km. However, the layer structures change with season because of variations in aerosol types and meteorological conditions, notably the south–north migration of the main transport corridor for the dust and biomass-burning outflow from Africa. In winter, dust is

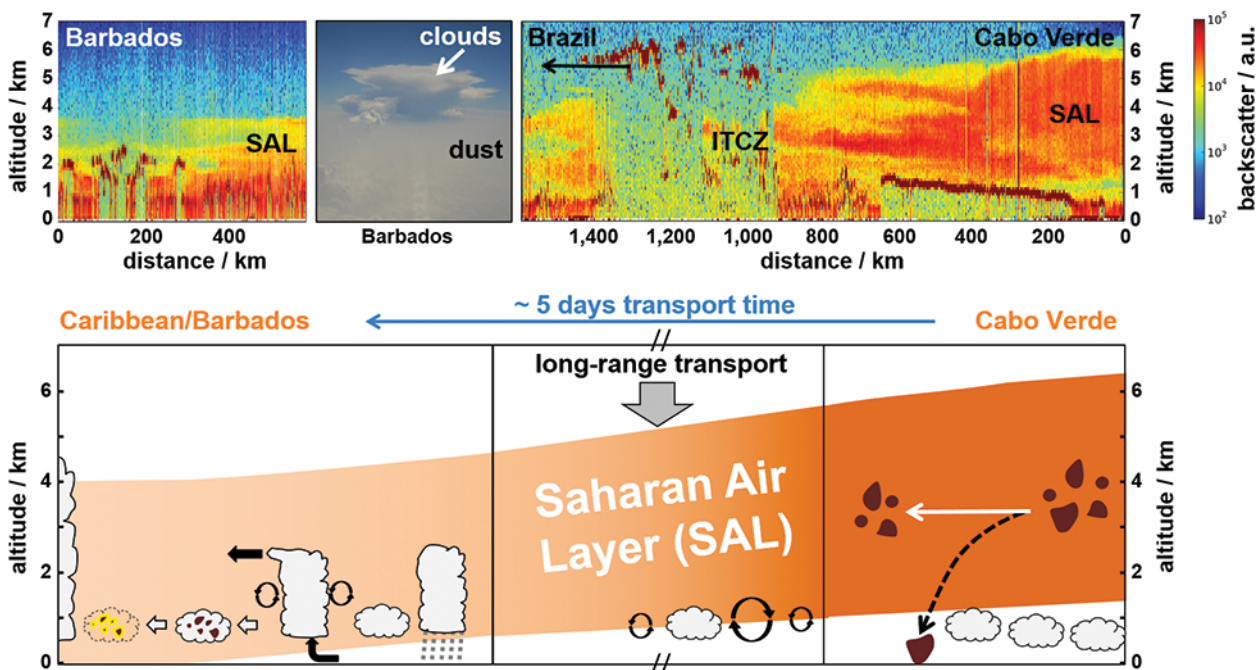


FIG. 6. (top) Lidar cross sections of dust-layer structure in (right) the Cabo Verde region and (left) Barbados together with (center) a photograph of dust layers in the Caribbean during SALTRACE in summer 2013. (bottom) Schematics of dust “aging” processes during transport from Africa into the Caribbean.

typically transported below 2-km altitude while biomass-burning dust mixtures are carried aloft; transport is primarily in latitudes south of Barbados which receives little aerosol during that time of year. In summer, the vertical aerosol distribution over Barbados shows three layers with different aerosol properties: 1) the boundary layer from the surface up to about 700 m where marine aerosols dominate; 2) above that, a layer of mixed mineral dust and marine aerosols reaching up to 1.5–2.5 km—this also is the height range where (mainly) trade wind cumulus clouds are present; and 3) the top layer extends from 1.5–2.5 to typically 4–5 km and is characterized by relatively pure Saharan dust. This layer contributes about half of the total optical depth at 532 nm (Groß et al. 2015).

Although we describe the transatlantic dust transport in simple terms, it should be clear that the processes are quite complex. Note, for example, that at Cabo Verde during summer, when transport to the Caribbean is at a maximum, there is very little dust in the marine boundary layer, which is dominated by

the low-level northeasterly trade wind flow. Transport takes place in the SAL above the measurement site. Similarly at Barbados in summer, the VLDR product would suggest that there is little dust in the boundary layer despite the fact that about 10–40 $\mu\text{g m}^{-3}$ of dust (Fig. 4) are present [for comparison: 50 $\mu\text{g m}^{-3}$ is the limit value for 24-h exposure to fine particulate matter (PM10) in the EU; <http://ec.europa.eu/environment/air/quality/standards.htm>]. This is a consequence of the boundary layer being heavily loaded with sea salt aerosol thus lowering the dust contribution to the total aerosol volume to about 30%–40% (Groß et al. 2016) and thereby decreasing the PLDR impact of dust.

HIGHLIGHTED SALTRACE RESULTS. In this section, we highlight three results from SALTRACE: The first example investigates the modification of mineral dust during transatlantic transport on the basis of a Lagrangian dust sampling experiment between Cabo Verde and Barbados. The second example presents the SALTRACE measurements

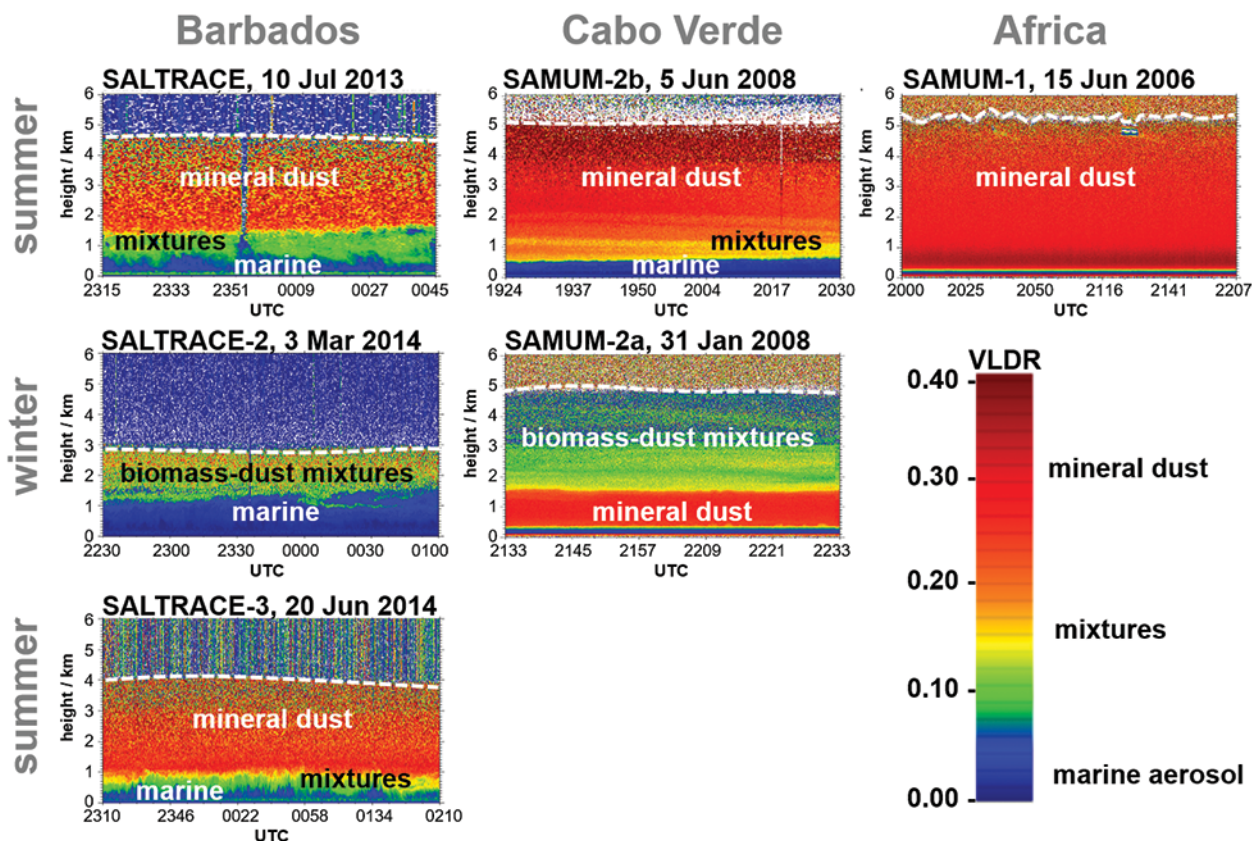


FIG. 7. Time–altitude cross sections of VLDR detected with the TROPOS lidar BERTHA at three different locations between Africa and the Caribbean (Ouarzazate, Morocco; Praia, Cabo Verde; and Barbados) in summer 2006, 2008, 2013, and 2014 and in winter 2008 and 2014. The aerosol extends from the ground to 3–5-km altitude. The top of the aerosol layers is indicated by the white dashed lines. Note: VLDR values in Morocco and Cabo Verde were measured at a wavelength of 710 nm, whereas the VLDR values in Barbados refer to 1,064 nm.

during the passage of Tropical Storm Chantal. The third example shows vertical profiles of lidar and in situ parameters for a case with high and low dust loads and discusses the SAL as a reservoir for CCN.

Modification of dust during transport across the Atlantic Ocean—A Lagrangian case study. One major objective of SALTRACE was to study the “aging” of dust during long-range transport and its impact on the radiation budget and cloud microphysical processes. This could be achieved by statistically comparing dust properties measured on the eastern Atlantic and later on the western Atlantic or by a Lagrangian experiment in which the same air mass is sampled multiple times on its trajectory as determined by means of meteorological models.

During SALTRACE we performed a Lagrangian experiment that studied dust in the Cabo Verde region

and 5 days later in the western Atlantic. We started with a series of north–south tracks in the Cabo Verde area on 17 June 2013. Flight legs at four different altitudes between 1 and 5 km were performed between the islands of Sal and Santiago, a distance of 210 km, roughly perpendicular to the dust outflow from the African continent. Before and after the flight, we ran trajectory and dispersion simulations with the Hybrid Single-Particle Lagrangian Integrated Trajectory model (HYSPLIT) (Draxler and Hess 1998) to predict when the sampled air would arrive over Barbados. This was determined to be on 22 June 2013. In the Caribbean, we carried out two flights on 20 and 21 June 2013, prior to the arrival of the Lagrangian-selected air mass. We performed the Lagrangian flight on 22 June 2013 where we flew on a north–south track along 59.5°W (i.e., perpendicular to the direction of propagation of the dust layer

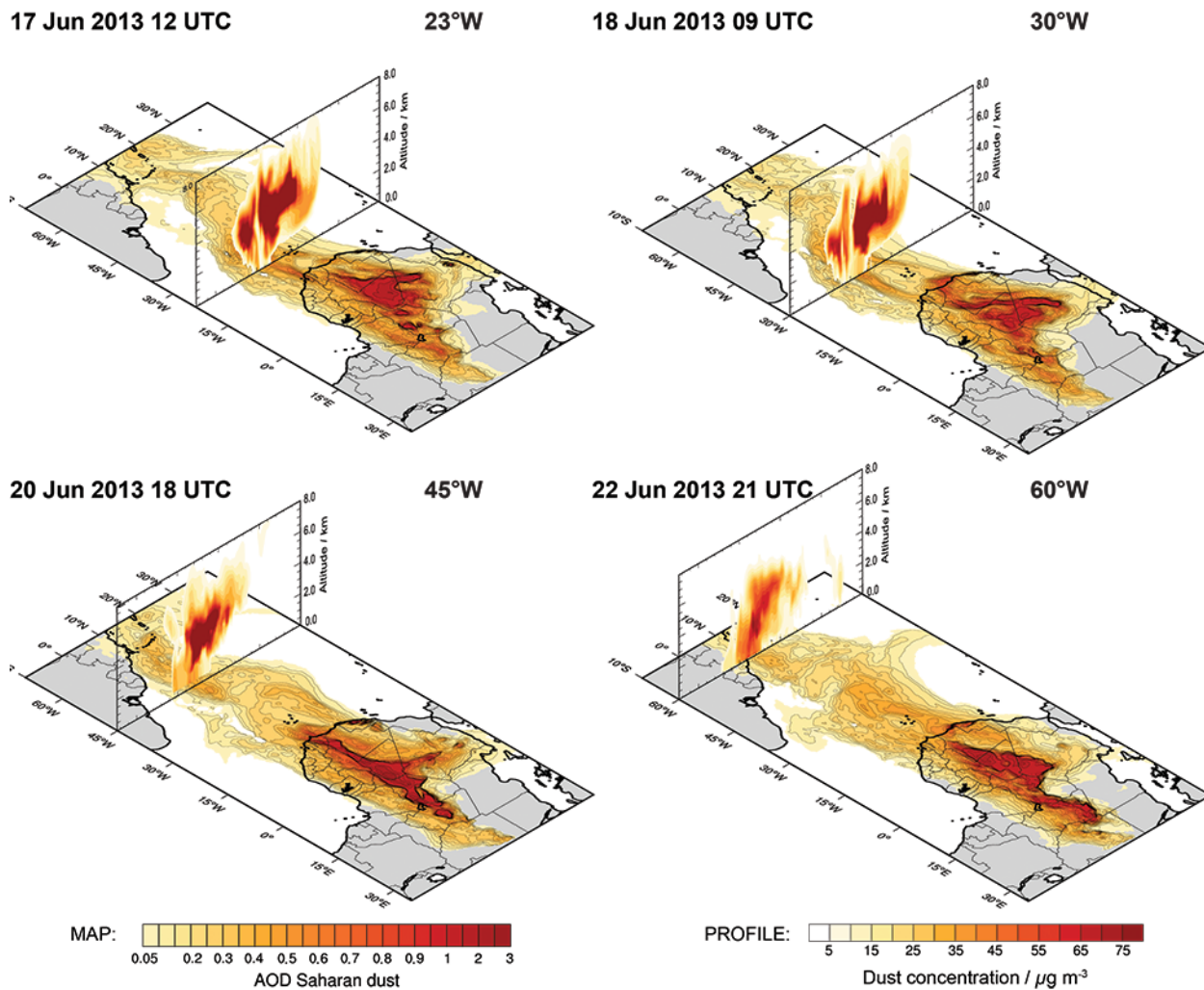


FIG. 8. COSMO-MUSCAT simulations showing the transatlantic dust transport for the Lagrangian dust sampling flights between 17 and 22 Jun 2013. Color-coded dust AOD maps are combined with longitude–altitude cross sections through the dust layer that show model dust mass concentrations.

from Africa to the Caribbean). The flight included several overpasses over Barbados at altitudes between 0.3 and 9 km and extended over a distance of ~470 km between 10.4° and 14.6°N. According to postcampaign analyses, the air mass sampled on 17 June 2013 at an altitude of 2.6 km in the Cabo Verde region was again sampled on 22 June 2013 over Barbados at an altitude of 2.3 km. It was above the typical scattered cloud layer extending from ~0.7 to 2 km on that day.

The Lagrangian experiment relies on a certain degree of homogeneity of the sampled air mass—a precondition that is satisfied by the well-mixed SAL. For example, the variability of the particle number concentration in the Lagrangian leg over Cabo Verde was below ~10% in the coarse mode (0.5–50 μm) and around 2% in the size range between 5 nm and <~2.5 μm over distances of more than 170 km.

Figure 8 visualizes the air mass transport of the Lagrangian experiment on the basis of Consortium for Small-Scale Modeling Multiscale Chemistry Aerosol Transport Model (COSMO-MUSCAT) simulations. COSMO-MUSCAT is a regional dust model system that computes the size-resolved distribution of Saharan dust including radiative effects and feedbacks (Heinold et al. 2007, 2011). Simulations were run for the period April–July 2013 with 28-km horizontal grid spacing on a model domain that covers the Saharan Desert and the tropical Atlantic Ocean including the Caribbean. Combined with trajectory analysis, COSMO-MUSCAT shows the relationship between the sampling areas at Cabo Verde and Barbados. According to these simulations, the predominant number of trajectories launched over Cabo Verde arrived at Barbados within a 250-km radius within the 5-day transport time.

The four panels in Fig. 8 illustrate the location and extent of the dust layer sampled on both sides of the Atlantic in the Lagrangian experiment as it crosses the Atlantic Ocean. Color-coded dust AOD maps

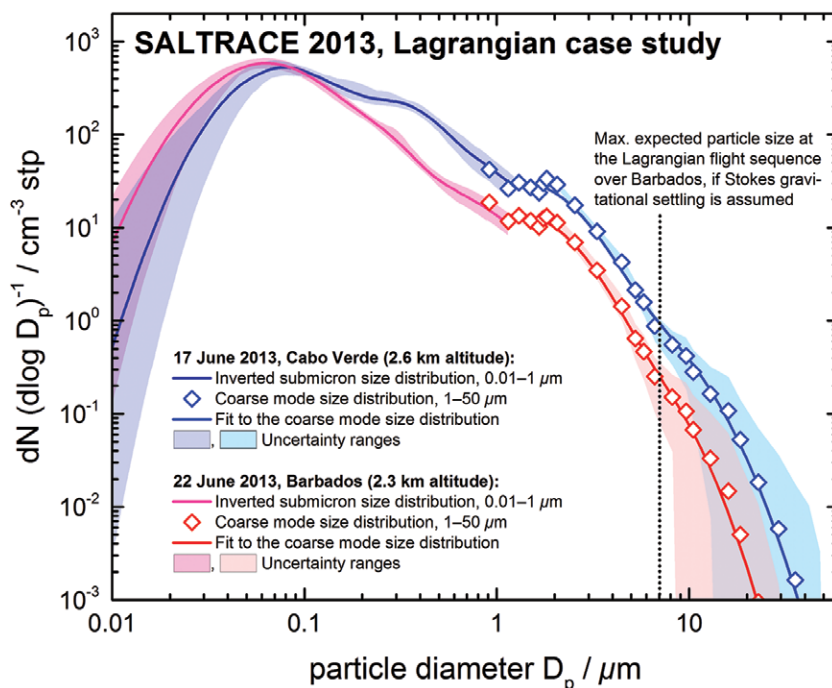


FIG. 9. Mineral dust size distribution detected with a combination of instruments before and after transatlantic transport: the size distribution between 0.01 and 1 μm was determined from the data of a CPC, a Grimm Sky OPC, and a UHSAS-A using a consistent Bayesian inversion procedure (Walser et al. 2017, manuscript submitted to *Atmos. Meas. Tech. Discuss.*); for the coarse mode above 1 μm, data points and uncertainty ranges from the CAS-DPOL spectrometer are shown. The air mass studied in the Cabo Verde region (blue symbols) on 17 Jun 2013 was sampled again 5 days later above Barbados (red symbols). According to Stokes gravitational settling, no particles larger than 7 μm should be present at an altitude of about 1.3 km below the SAL top (i.e., at the altitude where these measurements in Barbados were taken). Number concentrations are given for standard pressure and temperature conditions (1,013 hPa, 273 K).

are combined with longitude–altitude cross sections through the dust layer, which show model dust mass concentrations on 17, 18, 20, and 22 June 2013. The position and timing of maps and cross sections exactly correspond to the course of a 7-day forward trajectory starting over Cabo Verde (15.5°N, 23.3°W) on 17 June 2013 and computed with COSMO wind fields. During transport, the modeled dust-layer depth decreases from about 5 (Cabo Verde) to 4 km (Barbados area) and about half of the dust mass is removed. AERONET measurements in Cabo Verde and Barbados confirm a decrease in the AOD (500 nm) by a factor of about 2 from 0.54 to 0.26 during the 5 days. Similar results were obtained from the long-range transport study carried out based on the airborne Doppler wind lidar retrievals and model results of Monitoring Atmospheric Composition and Climate (MACC), the global aerosol model from European Centre for Medium-Range Weather Forecasts (Chouza et al. 2016a). Although MACC was

able to reproduce the general characteristics of the dust long-range transport process, important differences were observed in the dust vertical distribution and the African easterly jet intensity.

Figure 9 shows aerosol size distributions detected in Cabo Verde (blue symbols) at an altitude of 2.6 km and the corresponding measurements made 5 days later at an altitude of 2.3 km over Barbados (red symbols). The size distribution includes the total aerosol in the SAL and was detected with a combination of a condensation particle counter (CPC) and several optical particle counters (OPC). Detailed information about instruments used is given in Table ES1 in the supplemental material. Data from the CPC, the Grimm Sky OPC, and the Ultra Sensitivity Aerosol Spectrometer (UHSAS-A) were inverted with a consistent Bayesian inversion procedure and parameterized assuming three lognormal distributions following the method described following the method described in Walser et al. (2017, manuscript submitted to *Atmos. Meas. Tech. Discuss.*). The uncertainty range in the submicron size range reflects the uncertainty in the lognormal size distribution mode parameters. The supermicron size range was detected with a Cloud and Aerosol Spectrometer with Depolarization Detection (CAS-DPOL). The symbols show the mean values from the CAS-DPOL spectrometer, and the shaded areas indicate the standard deviation within the averaging interval. The complete size distribution (sub- and supermicron range) was parameterized with four lognormal distributions (solid lines).

Although in particular the coarse mode aerosol size range is associated with considerable uncertainties, changes are clearly visible in both total particle number concentration and number size distribution. With respect to particle number concentration in the size range between 100 nm and 50 μm , about 40% of all particles are “lost” during transatlantic transport. The number fraction of removed particles is size dependent and increases with increasing particles size. For example, in the size range between 1 and 10 μm about 60% of the particles are removed, whereas ~75% of the 10- μm particles, ~90% of the 20- μm and ~99% of the 30- μm particles are gone, suggesting that dry deposition is the dominating removal process at least during this case.

The detection of 10–30- μm particles in the Caribbean even after more than 4,000 km and 5 days of transport is unexpected. Although Maring et al. (2003) pointed out that Stokes gravitational settling overestimated the removal of particles smaller than 7.3 μm , they found that larger particles were effectively removed between Tenerife and Puerto

Rico. In contrast, Denjean et al. (2016) found that the modal peak diameter of the volume size distribution remained unvaried from one side of the Atlantic Ocean to the other (i.e., Cabo Verde to Puerto Rico) suggesting that after 2–3 days from uplift gravitational settling is practically ineffective. Assuming a density of 2.6 g cm⁻³ for dust and a shape factor of 1.4 (Hinds 1999) to account for the nonspherical particle shape, which slows down the settling velocity, a particle with 20 (30)- μm in diameter descends 2.1 (4.6) km day⁻¹. This means that even if 20 (30)- μm particles had been at the top of the SAL at an altitude of 6–7 km over Cabo Verde, they should have been removed from the atmosphere within 3 (1.5) days. The Barbados measurements shown in Fig. 9 were performed at 2.3-km altitude above ground and about 1.3 km below the SAL top. Assuming SAL transport without vertical shear, and thus a Stokes settling distance of 1.3 km for this measurement, the expected maximum particle size would be about 7 μm . In contrast, 20% (10%) of the 20 (30) μm survived in the dust layer and were observed over Barbados after 5 days of transport (Fig. 8), a fact that may have important implications for the dust radiative effects and the ability of particles to act as INP. To understand the presence of these supermicron particles, Gasteiger et al. (2017) investigated particle settling in the SAL from an integrated model, lidar, and in situ perspective. Although not claiming that their simplified model describes processes during long-range transport in detail, their model suggests that daytime convective mixing within the SAL would allow a fraction of particles with diameters of 20 μm and larger to arrive in the Caribbean.

During SALTRACE, we sampled particles on board the Falcon for offline-chemical analyses. For the Lagrangian case, approximately 3,000 particles were collected. These were analyzed by scanning electron microscopy and energy-dispersive x-ray spectroscopy (EDX) for size and composition and by transmission electron microscopy and EDX for volatility and composition. Particles were classified according to the chemical composition as described in Kandler et al. (2009) with the exception of quartz being classified as silicate. Volatility was determined according to a method previously described (Kandler et al. 2011; Kristensen et al. 2016).

Figure 10 shows the aerosol composition and volatility state before and after transatlantic transport for the Lagrangian case. The general composition with comparatively low calcium contents in the supermicron fraction is in line with the mainly southern Saharan/Sahelian sources (Scheuven et al. 2013). The change in composition at about 500-nm particle size after long-

range transport is more pronounced than in the dust-influenced Cabo Verde boundary layer (Kandler et al. 2011; Lieke et al. 2011) but less distinct than observed by chemical and microphysical measurements over the African continent (Kaaden et al. 2009; Kandler et al. 2009; Müller et al. 2009; Weinzierl et al. 2009).

Comparing the chemical composition before and after transport reveals an increase in the number abundance of soluble sulfates—most ammonium- and sodium-dominated sulfates—for submicron particles; also, there is a slightly increased abundance of particles internally mixed between silicate and sulfate. This is corroborated by the fact that the abundance of silicate particles with detectable amounts of sulfate (~1%) increased from 2.5% to 4.3%. For

supermicron particles, no considerable modification is visible, which is consistent with other recent observations in the Caribbean (Denjean et al. 2015). Also, the relative composition of the dust component with respect to different silicates (not shown) is indistinguishable before and after transport.

The volatility experiment for submicron particles reveals, in contrast, that there is an increase in both the amount of volatile material on the single particles and the abundance of totally volatile particles. The bottom panel of Fig. 10 shows the composition of the refractory residuals. Here, there is a clear increase in soot whereas dust decreases. Refractory material classified as “other” consists mainly of iron (probably oxides/hydroxides) and K-rich particles (perhaps

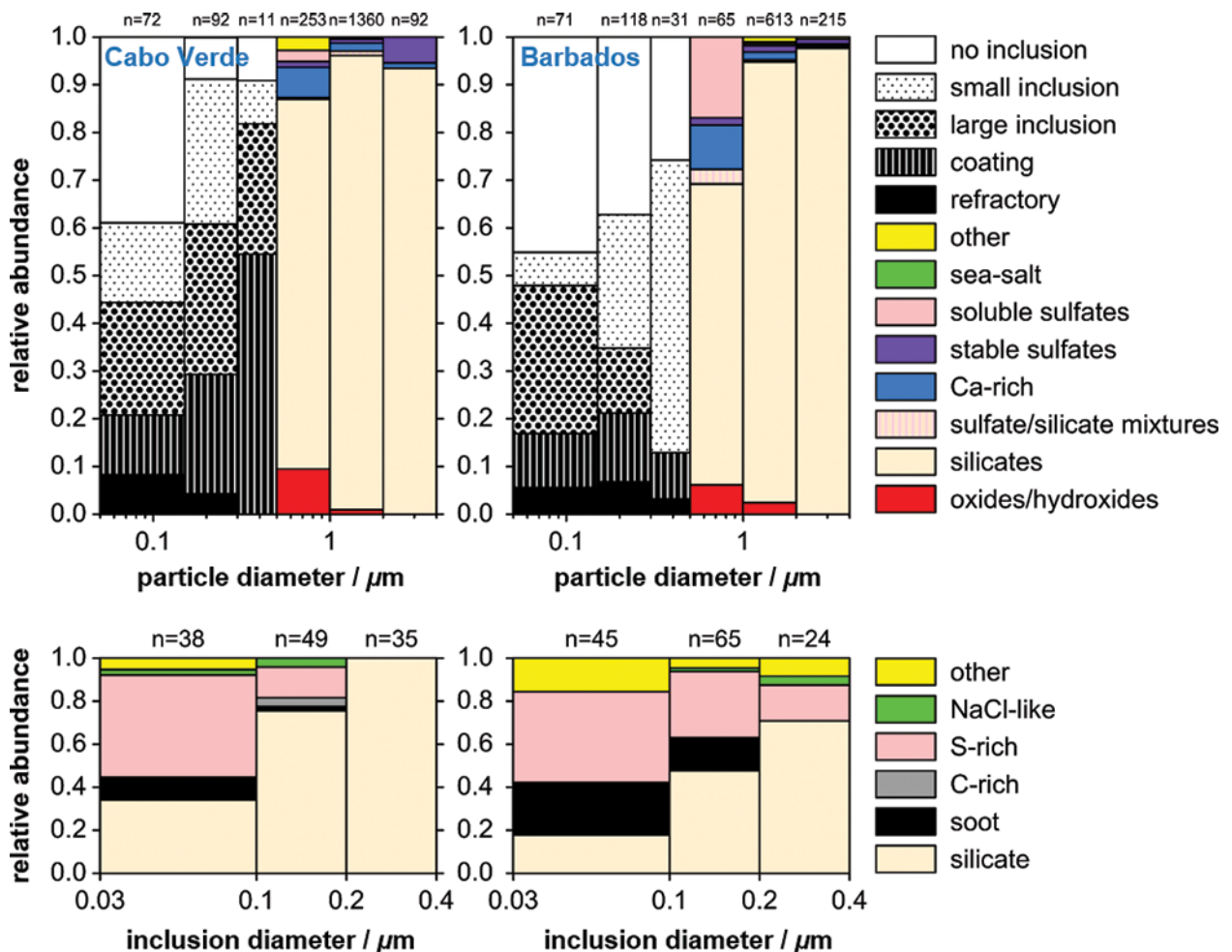


FIG. 10. Composition and volatility size distribution for the Lagrangian observations. The samples were collected (left) near Cabo Verde at 2.6-km altitude and (right) near Barbados at 2.3-km altitude. (top) Chemical particle groups are shown in color, and volatility observations are given in black and white (“small inclusion” referring to less than 30% of the particle volume, “large inclusion” to 30%–90%, and “coating” to more than 90% of the volume being refractory). (bottom) Composition of the refractory residuals with particle sizes given as projected area diameter. The numbers above the diagram are the particle counts for each bar; they cannot be considered as number size distribution.

biomass-burning material) (Lieke et al. 2011). The median volume fraction of volatile material internally mixed with soot is higher in transported aerosol (89% vs 79%). This volatile volume fraction for internally mixed dust particles does not change (7% vs 8%).

The passage of Tropical Storm Chantal and its impact on the Saharan air layer. During SALTRACE, we had the unique opportunity to perform extended aerosol measurements before, during, and after the passage of Tropical Storm Chantal, which evolved in an SAL environment. The SAL is attracting great interest because it is suspected to influence tropical cyclone activity (e.g., Dunion and Velden 2004; Evan et al. 2011). The observed modulation of the tropical Atlantic cyclone activity in the presence of the SAL

has been attributed to various causes. Evan et al. (2011) link weak cyclone activity to surface cooling through the radiative effects of the dust particles in the SAL. Furthermore, dust particles acting as CCN and INP might influence the development and formation of precipitation in the convective clouds and thus impact on the cyclone development. Local vertical wind shear can be enhanced by the midlevel jet found in the SAL, thereby hindering cyclone development (Dunion and Velden 2004).

Figure 11 (top) shows a time series of VLDR and range corrected backscatter for the period between 8 and 11 July 2013 detected with the Ludwig-Maximilians-Universität (LMU) Portable Lidar System (POLIS) (Freudenthaler et al. 2016) together with a map of the Meteosat SAL-tracking satellite

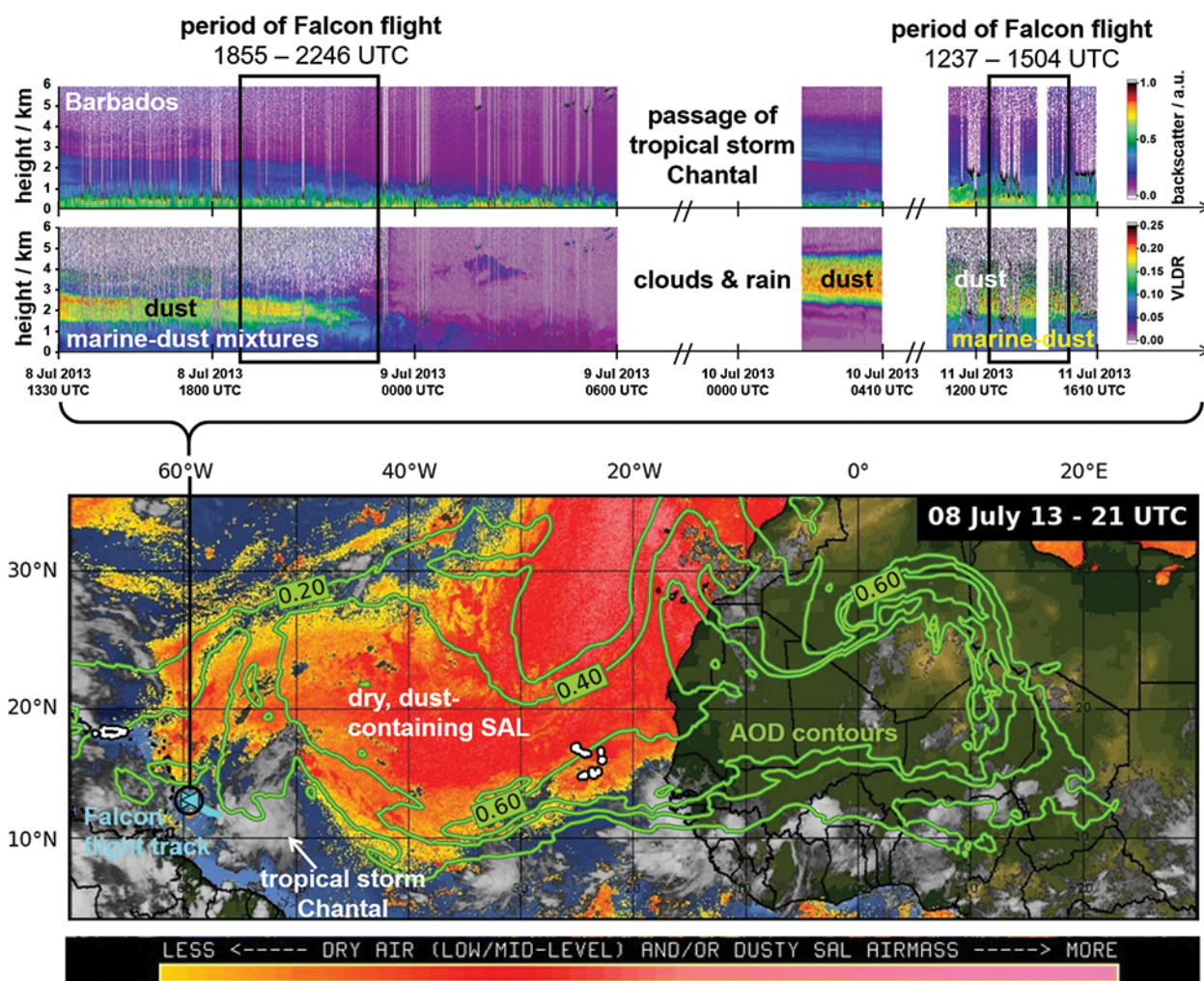


FIG. 11. (top) Measurements of VLDR (532 nm) and attenuated backscatter coefficient detected with the LMU lidar POLIS before, during, and after the passage of Tropical Storm Chantal, and on 11 Jul 2013 during the time of the first Falcon flight (Fig. 12). (bottom) Meteosat SAL-tracking satellite image (courtesy of the University of Wisconsin–Madison CIMSS) overlaid with contours of modeled dust AOD (500 nm, green contours) from the regional Saharan dust model COSMO-MUSCAT. The Falcon flight track is indicated in turquoise.

product, which we overlaid with contours of dust AOD from simulations with the regional dust model COSMO-MUSCAT. Both observations and regional dust simulations show that the passage of Chantal was associated with a reduced dust load in the Caribbean, which may largely be caused by mixing in clean air from farther south but also by wet removal of aerosols. This change in air mass is obvious from the SAL-tracking product (Fig. 11, bottom), while the analysis of dust model results including and without the storm event (not shown) reveals a minor role of wet deposition in the removal of dust. Vertical mixing was enhanced especially to the rear of the cyclone. Immediately after the passage of Chantal, changes in the dust properties were observed (Fig. 12) that might be linked to a change in the large-scale flow pattern over the tropical North Atlantic and West Africa, causing increased dust transport from southern Saharan and Sahelian dust sources. The dust layer was

seen to extend to about 5 km, higher than the typically observed 4–5 km. Details about DSA over North Africa and transported dust reaching Barbados are given in Groß et al. (2015). Future investigations will focus on the interactions of Tropical Storm Chantal and dust transport, including sensitivity studies on dust radiative effects and feedbacks on atmospheric dynamics and sea surface temperature.

The SAL as a reservoir/source for CCN. Here we highlight the vertical distribution of the microphysical properties of mineral dust and its ability to act as CCN. Mineral particles may serve as CCN in liquid cloud droplet formation (Sullivan et al. 2009; Garimella et al. 2014), and as such they are likely to be of great importance over the tropical Atlantic (Twohy et al. 2009). The efficacy of dust particles to act as CCN increases significantly with particle size, but it is also influenced by the presence of coatings and

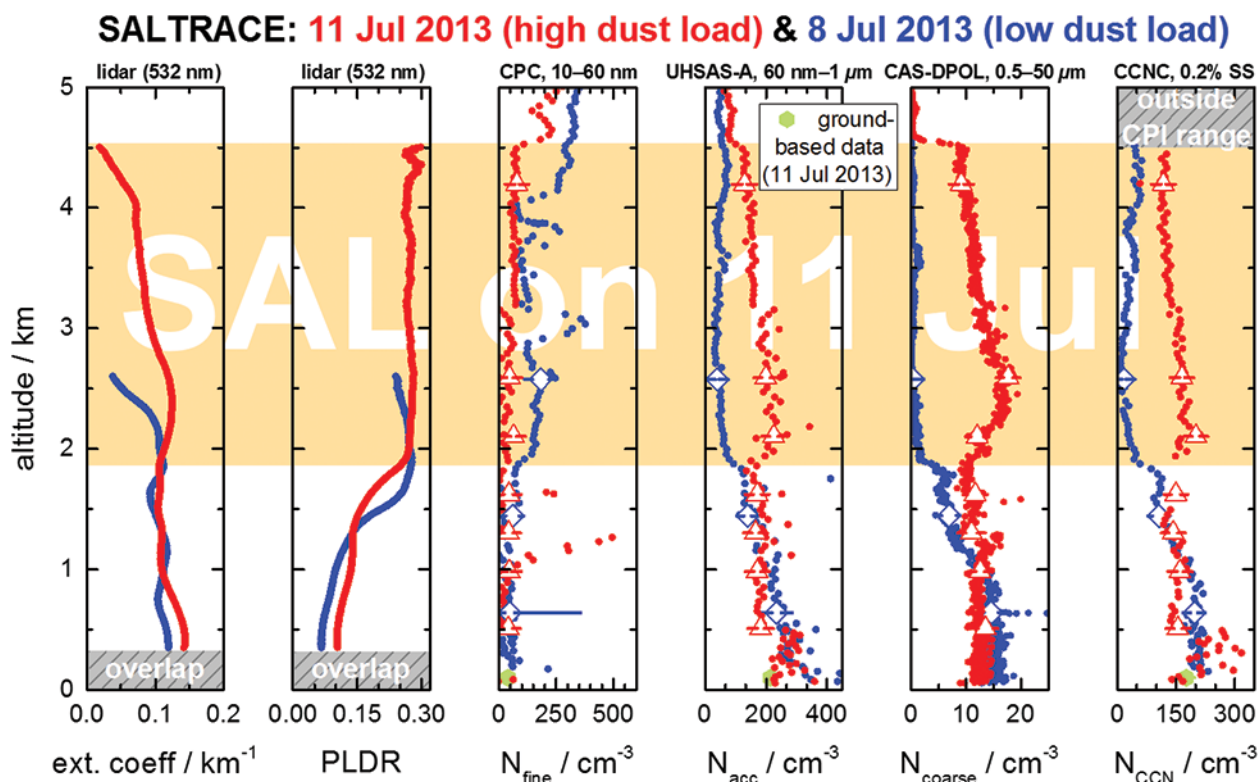


FIG. 12. Vertical profiles of extinction coefficient and PLDR detected with POLIS, aerosol number concentration detected with several instruments in different size classes, and CCN number concentration at 0.2% supersaturation (SS) for high (red) and low (blue) dust loads taken over Barbados on 8 and 11 Jul 2013 (see also Fig. 11 for the periods of the Falcon flights on those days). The corresponding ground-based measurements at Ragged Point are shown with green symbols. Data collected during sequences at constant altitude were averaged and are indicated with big symbols. The error bars indicate the 16th- and 84th-percentile values within the individual horizontal level. The gray-shaded areas sketch the overlap of the lidar and the range where the constant pressure inlet (CPI) of the CCN counter did no longer keep the CCNC at a constant pressure of 500 hPa. All data are given for ambient conditions.

the amount of (water soluble) coating material (e.g., Garimella et al. 2014). Pure mineral dust particles are hydrophobic, but if they are larger than $\sim 0.4\text{--}0.8\ \mu\text{m}$ they will act as CCN at atmospherically relevant supersaturations (Sullivan et al. 2009; Garimella et al. 2014). The addition of even minor amounts of water soluble material will increase the potential of dust particles to act as CCN (Sullivan et al. 2009). Furthermore, the addition of soluble material onto dust particles increases the water uptake at subsaturated conditions with respect to liquid water (Hatch et al. 2008) and, thus, influences their optical properties and the ability to scatter/absorb radiation.

Consequently, to assess the direct and indirect climate impacts from mineral particles, it is essential to investigate their mixing state and how that could change as the particles age in the atmosphere. Some studies indicate that processing of dust in the atmosphere leads to an addition of water soluble material (e.g., Perry et al. 2004; Begue et al. 2015). However, there have been only a few studies of the properties of aged African dust transported across the Atlantic. Denjean et al. (2015) investigated supermicron mineral dust particles sampled in Puerto Rico. They reported that up to 24% of the studied mineral dust particles were internally mixed with sulfate or chloride, while 3%–6% formed aggregates with sea salt particles. Only the latter group of mineral particles showed increased hygroscopic growth for relative humidity up to 94%.

Ground-based and airborne direct measurements of CCN concentrations were performed during SALTRACE. The potential of polarization lidar data to estimate vertical profiles of cloud-relevant aerosol parameters (CCN and INP number concentrations) was explored (Mamouri and Ansmann 2015). Furthermore, samples were collected for offline analysis of hygroscopic growth and ice nucleation ability.

Figure 12 contrasts vertical profiles of aerosol number concentration in different size classes together with the extinction coefficient measured with the ground-based lidar system from LMU Munich for days with high (11 July 2013) and low (8 July 2013) dust concentrations over Barbados. In addition, vertical profiles of PLDR enable us to distinguish the SAL pure dust layer that extends above about 1.5 (8 July) and 1.8 km (11 July) from the marine aerosol–dust mixture in the marine mixed layer. The particle number concentration in the fine mode (10–60 nm) seems to be depleted inside the SAL, while accumulation (60 nm– $1\ \mu\text{m}$) and coarse modes (0.5– $50\ \mu\text{m}$) are enhanced by a factor of more than 4

and 15, respectively, compared to free-tropospheric concentrations in these size ranges. The vertical profile of the CCN number concentration is correlated with accumulation and coarse mode number concentration. On the day with high dust loads, the CCN number concentration at altitudes of $\sim 2\text{--}4\ \text{km}$ is enhanced by a factor of about 5 compared to the day with the low dust load. Hence, it is likely that properties of clouds in the Caribbean formed at those altitudes are significantly influenced by long-range transported dust aerosol from northern Africa.

SUMMARY AND OUTLOOK. Although it is generally accepted that mineral dust affects many climate processes, our understanding of long-range transported dust is limited by the fragmentary nature of past studies. The strategy of SALTRACE was to attain a large-scale picture of African dust transport across the Atlantic by linking ground-based and airborne measurements with remote sensing and modeling. Specific objectives were 1) to characterize the chemical, microphysical, and optical properties of “aged” dust in the Caribbean, 2) to quantify the impact of dust “aging” on the radiation budget and cloud microphysical processes, 3) to investigate the meteorological context of African dust transport into the Caribbean, and 4) to assess the roles of removal processes during transport.

The SALTRACE program in 2013/14, especially with the aircraft field experiment in June and July 2013, comprised by far the most extensive measurements ever performed to study long-range transported dust. To our knowledge, the Lagrangian in situ study that sampled coherent air masses separated by a distance of more than 4,000 km was unique and enables a detailed investigation of transport effects on dust properties.

The Lagrangian results were surprising in that they suggest that the removal rate of large supermicron particles is slower than expected and the chemical alterations to the particles are less pronounced than expected. The exact nature of these aging processes is unclear and more research will be needed. The SALTRACE dataset enables future studies to look in detail at changes of chemical, microphysical, and optical dust properties during transport and quantify their associated effects on radiation and clouds.

To place the SALTRACE measurements in a long-term context we related our measurements to the 50-yr Barbados dust record and found that the situation investigated during SALTRACE can be regarded as “normal” dust conditions. Thus, the SALTRACE dataset is well suited to constrain the Atlantic and

Caribbean dust properties and concentrations in models. Temporal trends of ground-based dust mass concentrations and AOD at Barbados agreed well with aircraft measurements indicating that 1) mineral dust makes a significant contribution to the AOD in the Caribbean, 2) dust transported at higher altitudes into the Caribbean is effectively mixed down into the boundary layer, and 3) that in general we can expect good comparability between ground-based, airborne, and remote sensing observations.

We carried out extensive measurements in Tropical Storm Chantal, which developed when dust concentrations were high over broad areas of the western Atlantic. Chantal passed through the Barbados region on 9 July 2013. Interestingly, by the time the storm overpassed our ground site on Barbados essentially all dust was gone, an observation that we attribute to enhanced advection of dust-free air from the south. The SAL-tracking product and modeled dust AOD in Fig. 11 clearly show this change in air mass associated with the passage of storm Chantal.

We collected numerous in situ and remote sensing profiles of dust properties, which we evaluated with respect to their ability to act as CCN. We found the CCN number concentration in the SAL to be highly enhanced (~up to a factor of 5) under conditions of high dust loads compared to low dust loads.

The SALTRACE data should yield new insights on the formation (and destruction) of the dust-bearing SAL and its impact on cloud evolution processes, the atmospheric radiation budget, and local meteorology. Ongoing analyses are expected to elucidate details on the processes occurring at the end of the atmospheric dust cycle as the SAL moved over the Caribbean.

Simultaneous Doppler lidar backscatter and wind measurements were conducted for the first time along the main Saharan dust transport path. This unique dataset not only provides the opportunity to investigate various features associated with this transport but also to test the ability of different global and regional models to simulate them. Ongoing regional modeling will use the rich dataset to address fundamental questions on Saharan dust transport: how export across the tropical Atlantic is influenced by the West African circulation, the role played by the different removal and mixing processes, and the impact of dust on radiative forcing and on the dynamics of the SAL. Regional dust simulations and trajectory analysis will be used to explore deposition processes, particle aging, and dust–cloud interactions.

The role of dust as CCN and INP and the associated impacts on weather needs further research. The next generation of mineral dust field experiments

should focus on extended characterization of dust aerosol and include enhanced cloud observations (e.g., mixed-phase and ice clouds developing in dusty air layers) by combined in situ and remote sensing observations.

Finally, the long-term dust record from Barbados shows that large changes in transport have occurred and that these are clearly linked to climate in ways that we do not fully understand. In the coming decades we might expect continuing changes in global climate. However the projections for North Africa are highly uncertain and we cannot anticipate whether dust transport will increase or decrease (Seneviratne et al. 2012). Thus, it is important that dust transport out of Africa is carefully monitored in the coming years to better understand the controlling processes so as to develop better model projections of dust transport and the role of dust in a changing climate.

ACKNOWLEDGMENTS. The research leading to these results has received funding from the Helmholtz Association under Grant VH-NG-606 (Helmholtz-Hochschul-Nachwuchsforschergruppe AerCARE) and from the European Research Council under the European Community's Horizon 2020 research and innovation framework program/ERC Grant Agreement 640458 (A-LIFE). The SALTRACE campaign was mainly funded by the Helmholtz Association, DLR, TROPOS, and LMU. The SALTRACE flights in the Cabo Verde region were funded through the DLR-internal project VolcATS (Volcanic Ash Impact on the Air Transport System). We acknowledge funding from the LMU Munich's Institutional Strategy LMUexcellent within the framework of the German Excellence Initiative. The photometer calibration was supported by European Union's Horizon 2020 research and innovation program under Grant Agreement 654109 (ACTRIS-2). J. M. Prospero's research is supported by NSF Grant AGS-0962256. K. Kandler acknowledges financial support from the German Research Foundation (DFG, Grants KA 2280/2 and FOR 1525 INUIT). T. B. Kristensen thanks funding from the German Federal Ministry of Education and Research (BMBF) project 01LK1222B.

We thank the SALTRACE team and our local hosts for their support and the great collaboration. We are grateful to DLR flight experiments, in particular Andrea Hausold and Frank Probst; the pilots Stefan Grillenbeck, Michael Großrubatscher, Philipp Weber, Roland Welsler; and the technical and sensor team from DLR flight operations for their great support during the preparation of SALTRACE and for the accomplishment of the research flights. Special thanks due to the certification team of CAS-DPOL for enabling us to fly this instrument on the Falcon. We are grateful to the following participants of the SALTRACE field

experiment for their assistance before, during, and after the SALTRACE field phase: Reinhold Busen, Florian Dahlkötter, Daniel Fütterer, Markus Hartmann, Katharina Heimerl, André Klepel, Melanie Kujukovic, Christian Lemmerz, Anton Lex, Andreas Minikin, Engelbert Nagel, Stephan Rahm, Maximilian Rose, Meinhard Seefeldner, and Benjamin Witschas. Thanks are due to Andreas Dörnbrack, Robert Baumann, and Ingo Wenzel for preparing ECMWF and HYSPLIT trajectories and for their support with the weather forecast during SALTRACE. We thank Didier Tanré and LOA staff for their effort in establishing and maintaining Cabo Verde AERONET site and the Deutscher Wetterdienst (DWD) for good cooperation and support running the COSMO model and providing the required input data. We are grateful to the NASA CALIPSO team for providing CALIPSO data 3 h after downlink. Matthias Tesche kindly provided the SAMUM-1 and SAMUM-2 data in Fig. 8. We thank the University of Wisconsin–Madison CIMSS for providing the Meteosat SAL-layer tracking product.

SALTRACE would not have been possible without the excellent support from local authorities in Cabo Verde and Barbados including the Regional Security System (RSS), the Caribbean Institute for Meteorology and Hydrology (CIMH), and the Airport Authority GAIA (Grantley Adams International Airport Inc.), Barbados, who hosted us in their facilities and supported us to get clearances, which we gratefully acknowledge.

REFERENCES

Abdelkader, M., S. Metzger, R. E. Mamouri, M. Astitha, L. Barrie, Z. Levin, and J. Lelieveld, 2015: Dust–air pollution dynamics over the eastern Mediterranean. *Atmos. Chem. Phys.*, **15**, 9173–9189, doi:10.5194/acp-15-9173-2015.

Ansmann, A., and Coauthors, 2011: Saharan Mineral Dust Experiments SAMUM-1 and SAMUM-2: What have we learned? *Tellus*, **63B**, 403–429, doi:10.1111/j.1600-0889.2011.00555.x.

Atkinson, J. D., and Coauthors, 2013: The importance of feldspar for ice nucleation by mineral dust in mixed-phase clouds. *Nature*, **498**, 355–358, doi:10.1038/nature12278.

Balkanski, Y., M. Schulz, T. Claquin, and S. Guibert, 2007: Reevaluation of mineral aerosol radiative forcings suggests a better agreement with satellite and AERONET data. *Atmos. Chem. Phys.*, **7**, 81–95, doi:10.5194/acp-7-81-2007.

Begue, N., P. Tulet, J. Pelon, B. Aouizerats, A. Berger, and A. Schwarzenboeck, 2015: Aerosol processing and CCN formation of an intense Saharan dust plume during the EUCAARI 2008 campaign. *Atmos. Chem. Phys.*, **15**, 3497–3516, doi:10.5194/acp-15-3497-2015.

Brammer, A., and C. D. Thorncroft, 2015: Variability and evolution of African easterly wave structures and their relationship with tropical cyclogenesis over the eastern Atlantic. *Mon. Wea. Rev.*, **143**, 4975–4995, doi:10.1175/MWR-D-15-0106.1.

Braun, S. A., 2010: Reevaluating the role of the Saharan air layer in Atlantic tropical cyclogenesis and evolution. *Mon. Wea. Rev.*, **138**, 2007–2037, doi:10.1175/2009MWR3135.1.

Burton, S. P., and Coauthors, 2012: Aerosol classification using airborne High Spectral Resolution Lidar measurements—Methodology and examples. *Atmos. Meas. Tech.*, **5**, 73–98, doi:10.5194/amt-5-73-2012.

Carlson, T. N., and J. M. Prospero, 1972: The large-scale movement of Saharan air outbreaks over the northern equatorial Atlantic. *J. Appl. Meteor.*, **11**, 283–297, doi:10.1175/1520-0450(1972)011<0283:TLSMOS>2.0.CO;2.

Chouza, F., O. Reitebuch, S. Groß, S. Rahm, V. Freudenthaler, C. Toledano, and B. Weinzierl, 2015: Retrieval of aerosol backscatter and extinction from airborne coherent Doppler wind lidar measurements. *Atmos. Meas. Tech.*, **8**, 2909–2926, doi:10.5194/amt-8-2909-2015.

—, —, A. Benedetti, and B. Weinzierl, 2016a: Saharan dust long-range transport across the Atlantic studied by an airborne Doppler wind lidar and the MACC model. *Atmos. Chem. Phys.*, **16**, 11 581–11 600, doi:10.5194/acp-16-11581-2016.

—, —, M. Jähn, S. Rahm, and B. Weinzierl, 2016b: Vertical wind retrieved by airborne lidar and analysis of island induced gravity waves in combination with numerical models and in situ particle measurements. *Atmos. Chem. Phys.*, **16**, 4675–4692, doi:10.5194/acp-16-4675-2016.

Cotton, R. J., 2016: Ice in Clouds Experiment—Dust: A field campaign to study aerosol–cloud interactions. *Eighth Symp. on Aerosol–Cloud–Climate Interactions*, New Orleans, LA, Amer. Meteor. Soc., J5.3. [Available online at <https://ams.confex.com/ams/96Annual/webprogram/Paper282066.html>.]

Dahlkötter, F., and Coauthors, 2014: The Pagami Creek smoke plume after long-range transport to the upper troposphere over Europe—Aerosol properties and black carbon mixing state. *Atmos. Chem. Phys.*, **14**, 6111–6137, doi:10.5194/acp-14-6111-2014.

DeFlorio, M. J., I. D. Goodwin, D. R. Cayan, A. J. Miller, S. J. Ghan, D. W. Pierce, L. M. Russell, and B. Singh, 2016: Interannual modulation of subtropical Atlantic boreal summer dust variability by ENSO. *Climate Dyn.*, **46**, 585–599, doi:10.1007/s00382-015-2600-7.

Denjean, C., and Coauthors, 2015: Long-range transport across the Atlantic in summertime does not enhance

- the hygroscopicity of African mineral dust. *Geophys. Res. Lett.*, **42**, 7835–7843, doi:10.1002/2015GL065693.
- , and Coauthors, 2016: Size distribution and optical properties of mineral dust aerosols transported in the western Mediterranean. *Atmos. Chem. Phys.*, **16**, 1081–1104, doi:10.5194/acp-16-1081-2016.
- Doherty, O. M., N. Riemer, and S. Hameed, 2008: Saharan mineral dust transport into the Caribbean: Observed atmospheric controls and trends. *J. Geophys. Res.*, **113**, D07211, doi:10.1029/2007JD009171.
- Draxler, R. R., and G. D. Hess, 1998: An overview of the HYSPLIT_4 modeling system of trajectories, dispersion, and deposition. *Aust. Meteor. Mag.*, **47**, 295–308.
- Dunion, J. P., and C. S. Velden, 2004: The impact of the Saharan air layer on Atlantic tropical cyclone activity. *Bull. Amer. Meteor. Soc.*, **85**, 353–365, doi:10.1175/BAMS-85-3-353.
- Evan, A. T., A. K. Heidinger, and P. Knippertz, 2006: Analysis of winter dust activity off the coast of West Africa using a new 24-year over-water advanced very high resolution radiometer satellite dust climatology. *J. Geophys. Res.*, **111**, D12210, doi:10.1029/2005JD006336.
- , G. R. Foltz, D. X. Zhang, and D. J. Vimont, 2011: Influence of African dust on ocean–atmosphere variability in the tropical Atlantic. *Nat. Geosci.*, **4**, 762–765, doi:10.1038/ngeo1276.
- , C. Flamant, M. Gaetani, and F. Guichard, 2016: The past, present and future of African dust. *Nature*, **531**, 493–495, doi:10.1038/nature17149.
- Fitzgerald, E., A. P. Ault, M. D. Zauscher, O. L. Mayol-Bracero, and K. A. Prather, 2015: Comparison of the mixing state of long-range transported Asian and African mineral dust. *Atmos. Environ.*, **115**, 19–25, doi:10.1016/j.atmosenv.2015.04.031.
- Formenti, P., S. Caquineau, K. Desboeufs, A. Klaver, S. Chevaillier, E. Journet, and J. L. Rajot, 2014: Mapping the physico-chemical properties of mineral dust in western Africa: Mineralogical composition. *Atmos. Chem. Phys.*, **14**, 10663–10686, doi:10.5194/acp-14-10663-2014.
- Freudenthaler, V., and Coauthors, 2009: Depolarization ratio profiling at several wavelengths in pure Saharan dust during SAMUM 2006. *Tellus*, **61B**, 165–179, doi:10.1111/j.1600-0889.2008.00396.x.
- , M. Seefeldner, S. Groß, and U. Wandinger, 2016: Accuracy of linear depolarisation ratios in clean air ranges measured with POLIS-6 at 355 and 532 NM. *EPJ Web Conf.*, **119**, 25013, doi:10.1051/epjconf/201611925013.
- Garimella, S., Y. W. Huang, J. S. Seewald, and D. J. Cziczo, 2014: Cloud condensation nucleus activity comparison of dry- and wet-generated mineral dust aerosol: The significance of soluble material. *Atmos. Chem. Phys.*, **14**, 6003–6019, doi:10.5194/acp-14-6003-2014.
- Gasteiger, J., S. Groß, B. Weinzierl, D. Sauer, and V. Freudenthaler, 2017: Particle settling and convective mixing in the Saharan Air Layer as seen from an integrated model, lidar, and in-situ perspective. *Atmos. Chem. Phys.*, **17**, 297–311, doi:10.5194/acp-17-297-2017.
- Ginoux, P., J. M. Prospero, O. Torres, and M. Chin, 2004: Long-term simulation of global dust distribution with the GOCART model: Correlation with North Atlantic Oscillation. *J. Environ. Model. Software*, **19**, 113–128, doi:10.1016/S1364-8152(03)00114-2.
- Gioda, A., O. L. Mayol-Bracero, F. N. Scatena, K. C. Weathers, V. L. Mateus, and W. H. McDowell, 2013: Chemical constituents in clouds and rainwater in the Puerto Rican rainforest: Potential sources and seasonal drivers. *Atmos. Environ.*, **68**, 208–220, doi:10.1016/j.atmosenv.2012.11.017.
- Goudie, A. S., 2014: Desert dust and human health disorders. *Environ. Int.*, **63**, 101–113, doi:10.1016/j.envint.2013.10.011.
- Groß, S., M. Tesche, V. Freudenthaler, C. Toledano, M. Wiegner, A. Ansmann, D. Althausen, and M. Seefeldner, 2011: Characterization of Saharan dust, marine aerosols and mixtures of biomass burning aerosols and dust by means of multi-wavelength depolarization and Raman measurements during SAMUM-2. *Tellus*, **63B**, 706–724, doi:10.1111/j.1600-0889.2011.00556.x.
- , M. Esselborn, B. Weinzierl, M. Wirth, A. Fix, and A. Petzold, 2013: Aerosol classification by airborne high spectral resolution lidar observations. *Atmos. Chem. Phys.*, **12**, 25983–26028, doi:10.5194/acpd-12-25983-2012.
- , V. Freudenthaler, K. Schepanski, C. Toledano, A. Schäfler, A. Ansmann, and B. Weinzierl, 2015: Optical properties of long-range transported Saharan dust over Barbados as measured by dual-wavelength depolarization Raman lidar measurements. *Atmos. Chem. Phys.*, **15**, 11067–11080, doi:10.5194/acp-15-11067-2015.
- , J. Gasteiger, V. Freudenthaler, T. Müller, D. Sauer, C. Toledano, and A. Ansmann, 2016: Saharan dust contribution to the Caribbean summertime boundary layer—A lidar study during SALTRACE. *Atmos. Chem. Phys.*, **16**, 11535–11546, doi:10.5194/acp-16-11535-2016.
- Haarig, M., D. Althausen, A. Ansmann, A. Klepel, H. Baars, R. Engelmann, S. Groß, and V. Freudenthaler, 2016: Measurement of the linear depolarization ratio of aged dust at three wavelengths (355, 532 and 1064 nm) simultaneously over Barbados. *EPJ Web Conf.*, **119**, 18009, doi:10.1051/epjconf/201611918009.

- Hankes, I., Z. Wang, G. Zhang, and C. Fritz, 2015: Merger of African easterly waves and formation of Cape Verde storms. *Quart. J. Roy. Meteor. Soc.*, **141**, 1306–1319, doi:10.1002/qj.2439.
- Hatch, C. D., K. M. Gierlus, J. D. Schuttlefield, and V. H. Grassian, 2008: Water adsorption and cloud condensation nuclei activity of calcite and calcite coated with model humic and fulvic acids. *Atmos. Environ.*, **42**, 5672–5684, doi:10.1016/j.atmosenv.2008.03.005.
- Haywood, J. M., and Coauthors, 2008: Overview of the dust and biomass-burning experiment and African Monsoon Multidisciplinary Analysis special observing period-0. *J. Geophys. Res.*, **113**, D00C17, doi:10.1029/2008JD010077.
- , and Coauthors, 2011: Motivation, rationale and key results from the GERBILS Saharan dust measurement campaign. *Quart. J. Roy. Meteor. Soc.*, **137**, 1106–1116, doi:10.1002/qj.797.
- Heinold, B., J. Helmert, O. Hellmuth, R. Wolke, A. Ansmann, B. Marticorena, B. Laurent, and I. Tegen, 2007: Regional modeling of Saharan dust events using LM-MUSCAT: Model description and case studies. *J. Geophys. Res.*, **112**, D11204, doi:10.1029/2006JD007443.
- , and Coauthors, 2011: Regional modelling of Saharan dust and biomass-burning smoke. Part I: Model description and evaluation. *Tellus*, **63B**, 781–799, doi:10.1111/j.1600-0889.2011.00570.x.
- Heintzenberg, J. O. S. T., 2009: The SAMUM-1 experiment over southern Morocco: Overview and introduction. *Tellus*, **61B**, 2–11, doi:10.1111/j.1600-0889.2008.00403.x.
- Hinds, W. C., 1999: *Aerosol Technology: Properties, Behavior, and Measurement of Airborne Particles*. 2nd ed. Wiley, 504 pp.
- Hoose, C., and O. Möhler, 2012: Heterogeneous ice nucleation on atmospheric aerosols: A review of results from laboratory experiments. *Atmos. Chem. Phys.*, **12**, 9817–9854, doi:10.5194/acp-12-9817-2012.
- Huang, J. F., C. D. Zhang, and J. M. Prospero, 2010: African dust outbreaks: A satellite perspective of temporal and spatial variability over the tropical Atlantic Ocean. *J. Geophys. Res.*, **115**, D05202, doi:10.1029/2009JD012516.
- Huneeus, N., and Coauthors, 2011: Global dust model intercomparison in AeroCom phase I. *Atmos. Chem. Phys.*, **11**, 7781–7816, doi:10.5194/acp-11-7781-2011.
- IPCC, 2013: *Climate Change 2013: The Physical Science Basis*. Cambridge University Press, 1535 pp., doi:10.1017/CBO9781107415324.
- Jähn, M., D. Muñoz-Esparza, F. Chouza, O. Reitebuch, O. Knoth, M. Haarig, and A. Ansmann, 2016: Investigations of boundary layer structure, cloud characteristics and vertical mixing of aerosols at Barbados with large eddy simulations. *Atmos. Chem. Phys.*, **16**, 651–674, doi:10.5194/acp-16-651-2016.
- Jickells, T. D., and Coauthors, 2005: Global iron connections between desert dust, ocean biogeochemistry, and climate. *Science*, **308**, 67–71, doi:10.1126/science.1105959.
- Jung, E., B. Albrecht, J. M. Prospero, H. H. Jonsson, and S. M. Kreidenweis, 2013: Vertical structure of aerosols, temperature, and moisture associated with an intense African dust event observed over the eastern Caribbean. *J. Geophys. Res. Atmos.*, **118**, 4623–4643, doi:10.1002/jgrd.50352.
- Kaaden, N., and Coauthors, 2009: State of mixing, shape factor, number size distribution, and hygroscopic growth of the Saharan anthropogenic and mineral dust aerosol at Tinfou, Morocco. *Tellus*, **61B**, 51–63, doi:10.1111/j.1600-0889.2008.00388.x.
- Kandler, K., and Coauthors, 2009: Size distribution, mass concentration, chemical and mineralogical composition and derived optical parameters of the boundary layer aerosol at Tinfou, Morocco, during SAMUM 2006. *Tellus*, **61B**, 32–50, doi:10.1111/j.1600-0889.2008.00385.x.
- , and Coauthors, 2011: Electron microscopy of particles collected at Praia, Cape Verde, during the Saharan Mineral Dust Experiment: Particle chemistry, shape, mixing state and complex refractive index. *Tellus*, **63B**, 475–496, doi:10.1111/j.1600-0889.2011.00550.x.
- Kanitz, T., R. Engelmann, B. Heinold, H. Baars, A. Skupin, and A. Ansmann, 2014: Tracking the Saharan Air Layer with shipborne lidar across the tropical Atlantic. *Geophys. Res. Lett.*, **41**, 1044–1050, doi:10.1002/2013GL058780.
- Karyampudi, V. M., and T. N. Carlson, 1988: Analysis and numerical simulations of the Saharan Air Layer and its effect on easterly wave disturbances. *J. Atmos. Sci.*, **45**, 3102–3136, doi:10.1175/1520-0469(1988)045<3102:AANSOT>2.0.CO;2.
- Khan, B., G. Stenchikov, B. Weinzierl, S. Kalenderski, and S. Osipov, 2015: Dust plume formation in the free troposphere and aerosol size distribution during the Saharan Mineral Dust Experiment in North Africa. *Tellus*, **67B**, 27170, doi:10.3402/tellusb.v67.27170.
- Kiladis, G. N., C. D. Thorncroft, and N. M. J. Hall, 2006: Three-dimensional structure and dynamics of African easterly waves. Part I: Observations. *J. Atmos. Sci.*, **63**, 2212–2230, doi:10.1175/JAS3741.1.
- Knippertz, P., and M. C. Todd, 2010: The central west Saharan dust hot spot and its relation to African easterly

- waves and extratropical disturbances. *J. Geophys. Res.*, **115**, D12117, doi:10.1029/2009JD012819.
- Kristensen, T. B., T. Müller, K. Kandler, N. Benker, M. Hartmann, J. M. Prospero, A. Wiedensohler, and F. Stratmann, 2016: Properties of cloud condensation nuclei (CCN) in the trade wind marine boundary layer of the western North Atlantic. *Atmos. Chem. Phys.*, **16**, 2675–2688, doi:10.5194/acp-16-2675-2016.
- Kumar, P., I. N. Sokolik, and A. Nenes, 2011: Measurements of cloud condensation nuclei activity and droplet activation kinetics of fresh unprocessed regional dust samples and minerals. *Atmos. Chem. Phys.*, **11**, 3527–3541, doi:10.5194/acp-11-3527-2011.
- Levin, Z., E. Ganor, and V. Gladstein, 1996: The effects of desert particles coated with sulfate on rain formation in the eastern Mediterranean. *J. Appl. Meteor.*, **35**, 1511–1523, doi:10.1175/1520-0450(1996)035<1511:TEODPC>2.0.CO;2.
- Lieke, K., and Coauthors, 2011: Particle chemical properties in the vertical column based on aircraft observations in the vicinity of Cape Verde Islands. *Tellus*, **63B**, 497–511, doi:10.1111/j.1600-0889.2011.00553.x.
- Liu, Z., and Coauthors, 2008: CALIPSO lidar observations of the optical properties of Saharan dust: A case study of long-range transport. *J. Geophys. Res.*, **113**, D07207, doi:10.1029/2007JD008878.
- Maher, B. A., J. M. Prospero, D. Mackie, D. Gaiero, P. P. Hesse, and Y. Balkanski, 2010: Global connections between aeolian dust, climate and ocean biogeochemistry at the present day and at the last glacial maximum. *Earth-Sci. Rev.*, **99**, 61–97, doi:10.1016/j.earscirev.2009.12.001.
- Mahowald, N., S. Albani, J. F. Kok, S. Engelstaeder, R. Scanza, D. S. Ward, and M. G. Flanner, 2014: The size distribution of desert dust aerosols and its impact on the Earth system. *Aeolian Res.*, **15**, 53–71, doi:10.1016/j.aeolia.2013.09.002.
- Mamouri, R. E., and A. Ansmann, 2015: Estimated desert-dust ice nuclei profiles from polarization lidar: Methodology and case studies. *Atmos. Chem. Phys.*, **15**, 3463–3477, doi:10.5194/acp-15-3463-2015.
- Maring, H., D. L. Savoie, M. A. Izaguirre, L. Custals, and J. S. Reid, 2003: Mineral dust aerosol size distribution change during atmospheric transport. *J. Geophys. Res.*, **108**, 8592, doi:10.1029/2002JD002536.
- McConnell, C. L., and Coauthors, 2008: Seasonal variations of the physical and optical characteristics of Saharan dust: Results from the Dust Outflow and Deposition to the Ocean (DODO) experiment. *J. Geophys. Res.*, **113**, D14505, doi:10.1029/2007JD009606.
- Morman, S. A., and G. S. Plumlee, 2014: Dust and human health. *Mineral Dust: A Key Player in the Earth System*, P. Knippertz and W. J.-B. Stuut, Eds., Springer Netherlands, 385–409.
- Müller, D., and Coauthors, 2010: Mineral dust observed with AERONET Sun photometer, Raman lidar, and in situ instruments during SAMUM 2006: Shape-dependent particle properties. *J. Geophys. Res.*, **115**, D11207, doi:10.1029/2009JD012523.
- Müller, T., A. Schladitz, N. Kaaden, and A. Wiedensohler, 2009: Spectral absorption coefficients and imaginary parts of refractive indices of Saharan dust during SAMUM-1. *Tellus*, **61B**, 79–95, doi:10.1111/j.1600-0889.2008.00399.x.
- Myhre, G., and Coauthors, 2013: Anthropogenic and natural radiative forcing. *Climate Change 2013: The Physical Science Basis*, T. F. Stocker et al., Eds., Cambridge University Press, 659–740.
- Nickovic, S., A. Vukovic, M. Vujadinovic, V. Djurdjevic, and G. Pejanovic, 2012: Technical Note: High-resolution mineralogical database of dust-productive soils for atmospheric dust modeling. *Atmos. Chem. Phys.*, **12**, 845–855, doi:10.5194/acp-12-845-2012.
- Niedermeier, N., and Coauthors, 2014: Mass deposition fluxes of Saharan mineral dust to the tropical northeast Atlantic Ocean: An intercomparison of methods. *Atmos. Chem. Phys.*, **14**, 2245–2266, doi:10.5194/acp-14-2245-2014.
- Nousiainen, T., and K. Kandler, 2015: Light scattering by atmospheric mineral dust particles. *Light Scattering Reviews 9: Light Scattering and Radiative Transfer*, A. A. Kokhanovsky, Ed., Springer Berlin Heidelberg, 3–52.
- Otto, S., M. de Reus, T. Trautmann, A. Thomase, M. Wendisch, and S. Borrmann, 2007: Atmospheric radiative effects of an in-situ measured Saharan dust plume and the role of large particles. *Atmos. Chem. Phys.*, **7**, 4887–4903, doi:10.5194/acp-7-4887-2007.
- Peng, M. S., B. Fu, T. Li, and D. E. Stevens, 2012: Developing versus nondeveloping disturbances for tropical cyclone formation. Part I: North Atlantic. *Mon. Wea. Rev.*, **140**, 1047–1066, doi:10.1175/2011MWR3617.1.
- Perry, K. D., S. S. Cliff, and M. P. Jimenez-Cruz, 2004: Evidence for hygroscopic mineral dust particles from the Intercontinental Transport and Chemical Transformation Experiment. *J. Geophys. Res.*, **109**, D23S28, doi:10.1029/2004JD004979.
- Pöschl, U., 2005: Atmospheric aerosols: Composition, transformation, climate and health effects. *Angew. Chem., Int. Ed.*, **44**, 7520–7540, doi:10.1002/anie.200501122.
- Prospero, J. M., 1999: Long-range transport of mineral dust in the global atmosphere: Impact of African dust on the environment of the southeastern United

- States. *Proc. Natl. Acad. Sci. USA*, **96**, 3396–3403, doi:10.1073/pnas.96.7.3396.
- , and T. N. Carlson, 1972: Vertical and areal distribution of Saharan dust over western equatorial north Atlantic Ocean. *J. Geophys. Res.*, **77**, 5255–5265, doi:10.1029/JC077i027p05255.
- , and P. J. Lamb, 2003: African droughts and dust transport to the Caribbean: Climate change implications. *Science*, **302**, 1024–1027, doi:10.1126/science.1089915.
- , E. Bonatti, C. Schubert, and T. N. Carlson, 1970: Dust in the Caribbean atmosphere traced to an African dust storm. *Earth Planet. Sci. Lett.*, **9**, 287–293, doi:10.1016/0012-821X(70)90039-7.
- , F. X. Collard, J. Molinie, and A. Jeannot, 2014: Characterizing the annual cycle of African dust transport to the Caribbean Basin and South America and its impact on the environment and air quality. *Global Biogeochem. Cycles*, **28**, 757–773, doi:10.1002/2013GB004802.
- Raga, G. B., D. Baumgardner, and O. L. Mayol-Bracero, 2016: History of aerosol-cloud interactions derived from observations in mountaintop clouds in Puerto Rico. *Aerosol Air Qual. Res.*, **16**, 674–688, doi:10.4209/aaqr.2015.05.0359.
- Redelsperger, J.-L., C. D. Thorncroft, A. Diedhiou, T. Lebel, D. J. Parker, and J. Polcher, 2006: African Monsoon Multidisciplinary Analysis: An international research project and field campaign. *Bull. Amer. Meteor. Soc.*, **87**, 1739–1746, doi:10.1175/BAMS-87-12-1739.
- Reid, J. S., and Coauthors, 2003a: Comparison of size and morphological measurements of coarse mode dust particles from Africa. *J. Geophys. Res.*, **108**, 8593, doi:10.1029/2002JD002485.
- , and Coauthors, 2003b: Analysis of measurements of Saharan dust by airborne and ground-based remote sensing methods during the Puerto Rico Dust Experiment (PRIDE). *J. Geophys. Res.*, **108**, 8586, doi:10.1029/2002JD002493.
- Ryder, C. L., and Coauthors, 2015: Advances in understanding mineral dust and boundary layer processes over the Sahara from Fennec aircraft observations. *Atmos. Chem. Phys.*, **15**, 8479–8520, doi:10.5194/acp-15-8479-2015.
- Sassen, K., P. J. DeMott, J. M. Prospero, and M. R. Poellot, 2003: Saharan dust storms and indirect aerosol effects on clouds: CRYSTAL-FACE results. *Geophys. Res. Lett.*, **30**, 35–31, doi:10.1029/2003GL017371.
- Schepanski, K., I. Tegen, B. Laurent, B. Heinold, and A. Macke, 2007: A new Saharan dust source activation frequency map derived from MSG-SEVIRI IR-channels. *Geophys. Res. Lett.*, **34**, 1–5, doi:10.1029/2007GL030168.
- , —, M. C. Todd, B. Heinold, G. Bonisch, B. Laurent, and A. Macke, 2009: Meteorological processes forcing Saharan dust emission inferred from MSG-SEVIRI observations of subdaily dust source activation and numerical models. *J. Geophys. Res.*, **114**, D10201, doi:10.1029/2008JD010325.
- , —, and A. Macke, 2012: Comparison of satellite based observations of Saharan dust source areas. *Remote Sens. Environ.*, **123**, 90–97, doi:10.1016/j.rse.2012.03.019.
- Scheuven, D., L. Schütz, K. Kandler, M. Ebert, and S. Weinbruch, 2013: Bulk composition of northern African dust and its source sediments—A compilation. *Earth-Sci. Rev.*, **116**, 170–194, doi:10.1016/j.earscirev.2012.08.005.
- Schladitz, A., T. Müller, A. Massling, N. Kaaden, K. Kandler, and A. Wiedensohler, 2009: In situ measurements of optical properties at Tinfou (Morocco) during the Saharan Mineral Dust Experiment SAMUM 2006. *Tellus*, **61B**, 64–78, doi:10.1111/j.1600-0889.2008.00397.x.
- Schütz, L., 1980: Long-range transport of desert dust with special emphasis on the Sahara. *Ann. N. Y. Acad. Sci.*, **338**, 515–532, doi:10.1111/j.1749-6632.1980.tb17144.x.
- Seneviratne, S., and Coauthors, 2012: Changes in climate extremes and their impacts on the natural physical environment. *Managing the Risks of Extreme Events and Disasters to Advance Climate Change Adaptation*, C. B. Field et al., Eds., Cambridge University Press, 109–230.
- Siebert, H., and Coauthors, 2013: The fine-scale structure of the trade wind cumuli over Barbados—An introduction to the CARRIBA project. *Atmos. Chem. Phys.*, **13**, 10061–10077, doi:10.5194/acp-13-10061-2013.
- Smirnov, A., B. N. Holben, D. Savoie, J. M. Prospero, Y. J. Kaufman, D. Tanre, T. F. Eck, and I. Slutsker, 2000: Relationship between column aerosol optical thickness and in situ ground based dust concentrations over Barbados. *Geophys. Res. Lett.*, **27**, 1643–1646, doi:10.1029/1999GL011336.
- Sokolik, I. N., and Coauthors, 2001: Introduction to special section: Outstanding problems in quantifying the radiative impacts of mineral dust. *J. Geophys. Res.*, **106**, 18015–18028, doi:10.1029/2000JD900498.
- Spiegel, J. K., N. Buchmann, O. L. Mayol-Bracero, L. A. Cuadra-Rodriguez, C. J. Valle Díaz, K. A. Prather, S. Mertes, and W. Eugster, 2014: Do cloud properties in a Puerto Rican tropical montane cloud forest depend on occurrence of long-range transported African dust? *Pure Appl. Geophys.*, **171**, 2443–2459, doi:10.1007/s00024-014-0830-y.
- Stevens, B., and G. Feingold, 2009: Untangling aerosol effects on clouds and precipitation in a

- buffered system. *Nature*, **461**, 607–613, doi:10.1038/nature08281.
- , and Coauthors, 2016: The Barbados Cloud Observatory: Anchoring investigations of clouds and circulation on the edge of the ITCZ. *Bull. Amer. Meteor. Soc.*, **97**, 787–801, doi:10.1175/BAMS-D-14-00247.1.
- Sullivan, R. C., M. J. K. Moore, M. D. Petters, S. M. Kreidenweis, G. C. Roberts, and K. A. Prather, 2009: Effect of chemical mixing state on the hygroscopicity and cloud nucleation properties of calcium mineral dust particles. *Atmos. Chem. Phys.*, **9**, 3303–3316, doi:10.5194/acp-9-3303-2009.
- Swap, R., M. Garstang, S. Greco, R. Talbot, and P. Kallberg, 1992: Saharan dust in the Amazon basin. *Tellus*, **44B**, 133–149, doi:10.1034/j.1600-0889.1992.t01-1-00005.x.
- Tanré, D., and Coauthors, 2003: Measurement and modeling of the Saharan dust radiative impact: Overview of the Saharan Dust Experiment (SHADE). *J. Geophys. Res.*, **108**, 8574, doi:10.1029/2002JD003273.
- Tegen, I., 2003: Modeling the mineral dust aerosol cycle in the climate system. *Quat. Sci. Rev.*, **22**, 1821–1834, doi:10.1016/S0277-3791(03)00163-X.
- Tesche, M., A. Ansmann, D. Müller, D. Althausen, R. Engelmann, V. Freudenthaler, and S. Gross, 2009: Vertically resolved separation of dust and smoke over Cape Verde using multiwavelength Raman and polarization lidars during Saharan Mineral Dust Experiment 2008. *J. Geophys. Res.*, **114**, D13202, doi:10.1029/2009JD011862.
- , and Coauthors, 2011: Optical and microphysical properties of smoke over Cape Verde inferred from multiwavelength lidar measurements. *Tellus*, **63B**, 677–694, doi:10.1111/j.1600-0889.2011.00549.x.
- Thorncroft, C. D., and M. Blackburn, 1999: Maintenance of the African easterly jet. *Quart. J. Roy. Meteor. Soc.*, **125**, 763–786, doi:10.1002/qj.4971255502.
- Toledano, C., and Coauthors, 2011: Optical properties of aerosol mixtures derived from sun-sky radiometry during SAMUM-2. *Tellus*, **63B**, 635–648, doi:10.1111/j.1600-0889.2011.00573.x.
- Twohy, C. H., and Coauthors, 2009: Saharan dust particles nucleate droplets in eastern Atlantic clouds. *Geophys. Res. Lett.*, **36**, L01807, doi:10.1029/2008GL035846.
- Valle-Díaz, C. J., E. Torres-Delgado, S. M. Colon-Santos, T. Lee, J. L. Collett, W. H. McDowell, and O. L. Mayol-Bracero, 2016: Impact of long-range transported African dust on cloud water chemistry at a tropical montane cloud forest in northeastern Puerto Rico. *Aerosol Air Qual. Res.*, **16**, 653–664, doi:10.4209/aaqr.2015.05.0320.
- Wang, C., S. Dong, A. T. Evan, G. R. Foltz, and S.-K. Lee, 2012: Multidecadal covariability of North Atlantic sea surface temperature, African dust, Sahel rainfall, and Atlantic hurricanes. *J. Climate*, **25**, 5404–5415, doi:10.1175/JCLI-D-11-00413.1.
- Wang, W., A. T. Evan, C. Flamant, and C. Lavaysse, 2015: On the decadal scale correlation between African dust and Sahel rainfall: The role of Saharan heat low–forced winds. *Sci. Adv.*, **1**, e1500646, doi:10.1126/sciadv.1500646.
- Washington, R., and Coauthors, 2012: Fennec—The Saharan climate system. *CLIVAR Exchanges*, No. 60, International CLIVAR Project Office, Southampton, United Kingdom, 31–32. [Available online at www.clivar.org/sites/default/files/documents/Exchanges60.pdf.]
- Weinzierl, B., and Coauthors, 2009: Airborne measurements of dust layer properties, particle size distribution and mixing state of Saharan dust during SAMUM 2006. *Tellus*, **61B**, 96–117, doi:10.1111/j.1600-0889.2008.00392.x.
- , and Coauthors, 2011: Microphysical and optical properties of dust and tropical biomass burning aerosol layers in the Cape Verde region—An overview of the airborne in-situ and lidar measurements during SAMUM-2. *Tellus*, **63B**, 589–618, doi:10.1111/j.1600-0889.2011.00566.x.
- , and Coauthors, 2012: On the visibility of airborne volcanic ash and mineral dust from the pilot’s perspective in flight. *Phys. Chem. Earth*, **45–46**, 87–102, doi:10.1016/j.pce.2012.04.003.
- Wurzler, S., T. G. Reisin, and Z. Levin, 2000: Modification of mineral dust particles by cloud processing and subsequent effects on drop size distributions. *J. Geophys. Res.*, **105**, 4501–4512, doi:10.1029/1999JD900980.
- Yu, H. B., and Coauthors, 2015: Quantification of trans-Atlantic dust transport from seven-year (2007–2013) record of CALIPSO lidar measurements. *Remote Sens. Environ.*, **159**, 232–249, doi:10.1016/j.rse.2014.12.010.
- Zipsper, E. J., and Coauthors, 2009: The Saharan Air Layer and the fate of African easterly waves. *Bull. Amer. Meteor. Soc.*, **90**, 1137–1156, doi:10.1175/2009BAMS2728.1.

AMS Education offers a new format option to view the AMS undergraduate course ebooks.

The WEBBOOK IS HERE!



- ✓ Read with any web browser
- ✓ Accessible anywhere with internet access
- ✓ Accessible on public computers
- ✓ Ideal for labs with computers
- ✓ Contains dynamic web-based features
- ✓ Allows student highlighting and notetaking

ametsoc.org/webBooks